PRACTICAL IMPLEMENTATION OF TORSIONAL ANALYSIS AND FIELD MEASUREMENT

Malcolm E. Leader, P.E.
Applied Machinery Dynamics Co.
P.O. BOX 157
Dickinson, TX 77539
MLeader@RotorBearingDynamics.COM

Ray D. Kelm, P.E.
Kelm Engineering
104 W. Myrtle Suite 201
Angleton, TX 77515
Ray@KelmEngineering.COM

Abstract: This paper is intended as a "nuts-and-bolts" approach to torsional analysis. Basic methods are detailed including how to calculate the stiffness and inertia of machine parts. Simple 2-mass and 3-mass systems are illustrated as well as complex systems that must be computer modeled. Forced response of torsional systems is investigated and several case studies are presented. Torsional analysis problems can become extremely complicated and theoretical modeling often must be tempered with actual field measurements. This way system modifications can be made with greater certainty of success. Various methods of measuring torsional vibration frequency and amplitude are presented; some that are accurate. Correlation to a mathematical model and solutions to torsional problems are presented. Several case histories are detailed and references to other torsional analysis material is provided.

Key Words: Damping; Experimental; Forced Response; Modeling; Properties; Testing; Torsional; Vibration

Introduction: While a minimum of two inertias connected by a spring (e.g. a motor driving a fan through a flexible coupling) are required, torsional analysis of rotating equipment is less complicated than lateral analysis. Torsionally it is easier to simplify the mechanical parts of a machine train into stiffnesses and inertias. Bearings and damping have little effect on the calculations. For simple systems, closed form equations often suffice to yield accurate torsional resonant frequency values. It can be difficult to obtain accurate inertia values of complex geometries like centrifugal impellers but these can also be measured experimentally. The torsional stiffness values of flexible couplings are available from the manufacturers. Elastomeric couplings are sometimes applied and introduce non-linear elements into the analysis. Gears may have backlash that can introduce additional non-linear effects.

Many different mechanisms can excite torsional resonances in rotating equipment trains. Some examples of prime movers that produce torque pulsations are synchronous motors, variable frequency drives and reciprocating engines. Speed changing gears also can produce torque pulsations. The driven equipment may also be a torsional exciter as with positive displacement pumps and compressors or blade-pass frequencies in centrifugal equipment. This paper uses English units and includes a unit conversion chart.

Basic Torsional Information: In order to begin torsional modeling of a rotating equipment train, the system geometry must be known. It is possible to do a lumped parameter analysis where the total inertia of the main components are connected by single-value stiffness springs. However, this approach is often inaccurate as it relies on the calculations of others and should only be done as a last resort. It is much better if the analyst has access to the complete system geometry and simplifies judiciously. Improper modeling is very difficult to detect without access to raw data and the assumptions of the analyst.

The most basic data required for the analysis is the polar moment of inertia, **J**. Figure 1 shows a simple circular disk that would be mounted to a shaft.

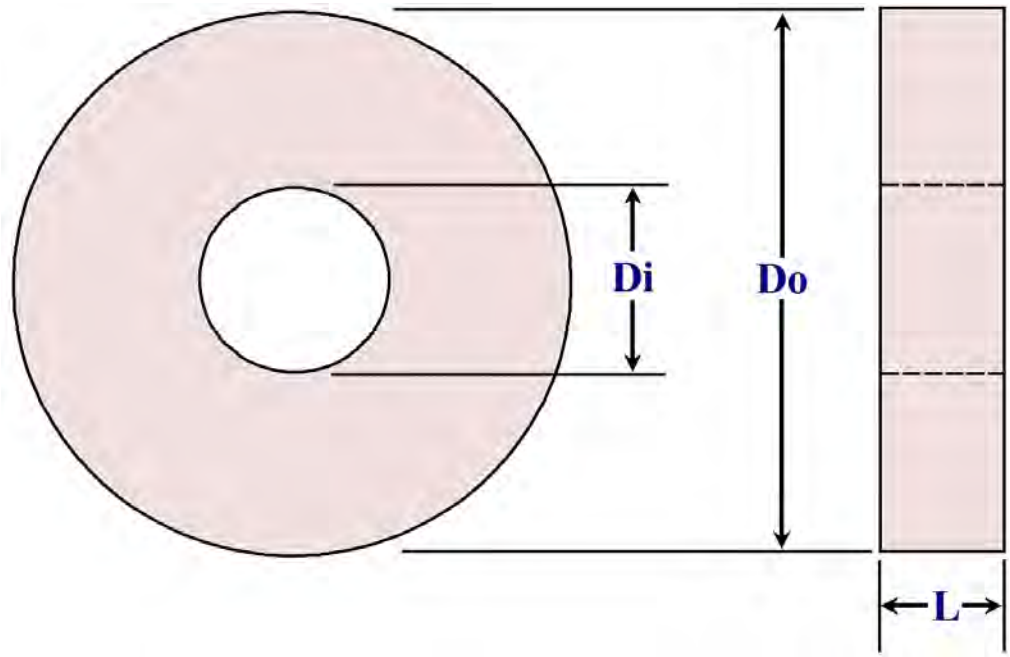

Figure 1 - Geometry of Simple Uniform Circular Disk

$$J = \frac{\rho \ \pi \ L \ (Do^4 - Di^4)}{32} \quad ; \rho = Density \qquad \text{Eq. 1}$$

If the weight of the part is known the polar inertia is:

$$J = Weight \ \frac{(Do^2 + Di^2)}{8} \qquad \text{Eq. 2}$$

If the disk is not a solid object, but rather something like an impeller, calculating the polar moment of inertia can be difficult. There are a number of ways to determine the correct values. Sometimes the manufacturer will provide the data. A previous lateral or torsional analysis may be available, or it can be determined experimentally. A good estimate for the density, ρ in Eq. 1, for closed centrifugal impellers is 21 to 25 percent of the actual material density. For open impellers, the estimated density can range from 15 to 25 percent depending on the construction and complexity of the vanes. It helps to accumulate a file of known impeller properties. If an impeller is available to be measured, there are CAD programs that will calculate the inertia. For reciprocating parts, the polar inertia is one-half the reciprocating mass times the radial throw squared.

Often the total polar inertia of a rotor is available from the manufacturer. If this value is not available and if a complete rotor is available, the total rotor inertia can be determined using a method developed by Michael Calistrat. This method involves mounting the rotor in rollers like a balance machine. Then a thin wire (radius **r**) is wrapped around the rotor (radius **R**) several times. On the free end of the wire, just enough weight is added to start the rotor turning in the rollers. This weight is the amount required to overcome friction. Then additional weight ($\mathbf{W_{Test}}$) is added and released. The time, **t**, for the weight to drop a measured distance, $\mathbf{D}_f$ (2 feet is a good one to use) is then measured. This should be repeated several times to assure repeatability. The times are then averaged and Eq. 3 is used to calculate the total inertia of the rotor. This method takes a little practice and it is recommended that some expertise be developed on a rotor with a known inertia or a bare shaft for which the inertia can be calculated exactly. Once the total rotor inertia is determined, the inertia of impellers or other attachments like motor windings can be calculated by subtracting those parts whose inertia can be calculated.

$$J_{Total} = W_{Test} \; (R_{Rotor} + r_{Wire}) \left(\frac{t^2}{2\, D_f} - \frac{1}{386.088} \right) \quad LB\text{-}IN\text{-}SEC^{\,2} \qquad \text{Eq. 3}$$

There is also an experimental way to determine the polar inertia of components like impellers and other irregular parts. This method involves hanging a platform from the ceiling with three thin wires at a precise radius **R** from the exact center of the platform as shown in figure 2. The weight of the table and the test piece weight must be known. Their combined weight is $\mathbf{W_T}$. It is easy to calibrate this test with a disk of known inertia.

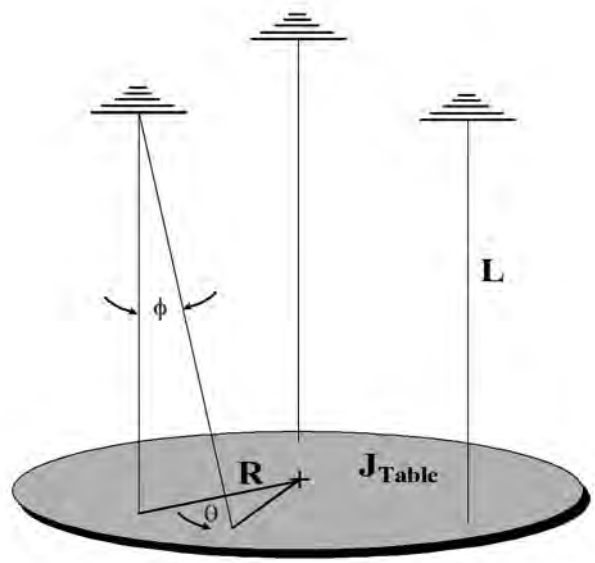

Figure 2

The wires should be as long as possible to minimize error. The table is usually made of sheet metal capable of supporting the parts to be measured. The inertia of the table by itself can be determined from Eq. 1. A part is very carefully centered on the table and given an initial angular displacement, θ, <u>less than 5 degrees</u>. Once released the assembly will oscillate and the frequency, ***f*** in cycles-per-second, of the oscillation is measured over 10 or more cycles. Using Eq. 4 the total inertia of the table plus the test piece is determined.

$$J_{TOTAL} = \frac{R^2 \; W_T}{4 \; \pi^2 \; L \; f^2} \qquad \text{Eq. 4}$$

Then the inertia of the table ($\mathbf{J_{Table}}$) is subtracted to attain the inertia of the test piece. The English units of polar inertia resulting from this test will be LB-IN-SEC^2.

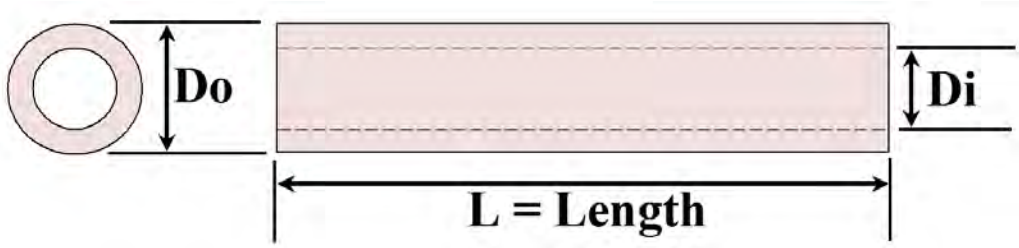

Figure 3 - Torsional Stiffness

The other primary information required for torsional analysis is the stiffness of the connections between inertias. If these sections are circular shafting as shown in figure 3, then Eq. 5 will provide the required values.

In this equation Φ is the twist angle in radians that results from an applied torque, **T**. $\mathbf{I_P}$ is the polar moment if inertia $\mathbf{[\pi(Do^4 - Di^4)/32]}$ and **G** is the shear modulus of the material. **G** is approximately 11.6 X 10^6 PSI for steel.

$$\Phi = \frac{T\,L}{I_P\,G} \quad \therefore \quad K_T = \frac{T}{\Phi} = \frac{I_P\,G}{L} \qquad \frac{IN\text{-}LB}{RAD} \qquad \text{Eq. 5}$$

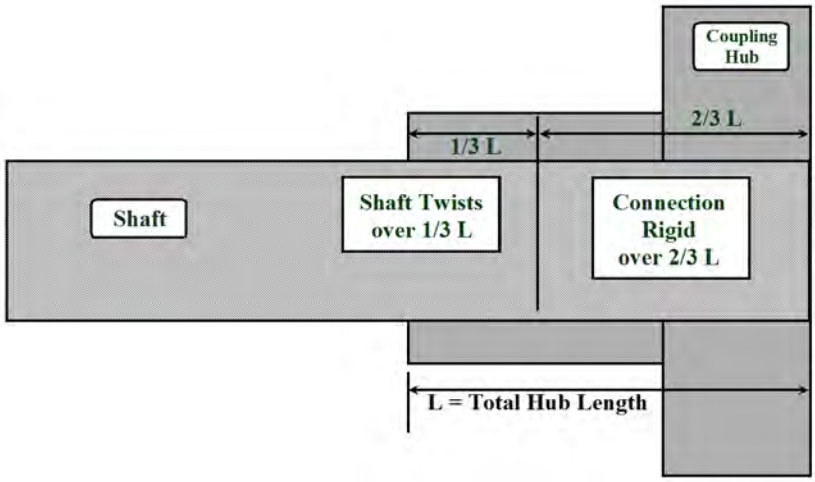

Figure 4 - Shaft Penetration Effect

In order to determine the torsional stiffness for non-circular or complicated geometries, such as a crankshaft, one of the references should be consulted. Mounted components, particularly those with an interference fit, alter the effective torsional stiffness of that section. This is often seen with mounted coupling hubs as illustrated in figure 4. This shows a shrink length, **L**, and it is assumed, based on testing, that one-third of the shaft penetration under the hub is free to turn and two-thirds is not. This technique is for typical mechanical mounting practices in the rotating equipment industry. There are more precise methods of determining the exact penetration effect (available in reference 1), but they are rarely necessary in this author's opinion. For keyed parts with little interference the penetration effect is approximately one-half of the total length. The softest torsional members in a rotating equipment train are usually the flexible couplings. The torsional stiffness values supplied by the coupling manufacturers almost always include the ⅓ penetration effect.

It must be noted that penetration effects also exist where shaft diameter changes take place in the torque path. As torque "flows" from one diameter section to the next, there is a slight decrease in effective diameter at the change in diameters because the torque does not radiate to the corners of the larger diameter. Several of the references have detailed information on how to incorporate this effect into the calculations. The authors usually does not consider this effect unless the diameter change is greater than 2 to 1 as the frequency calculation results are altered by less than one percent.

Modeling of Equipment Trains: Once each rotor in a train has been defined, a calculation method is selected. The easiest method is the lumped inertia and spring method as illustrated in figure 5.

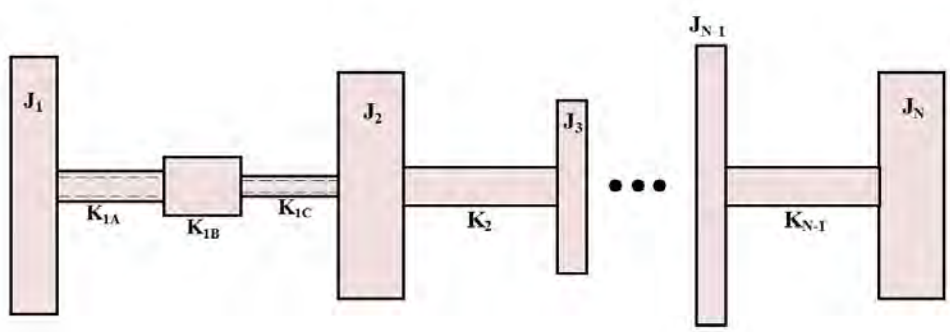

Figure 5 - Lumped Stiffness and Inertia Modeling

Determining the stiffnesses between inertias is a process of summing the stiffnesses of each shaft section. In figure 5 the shafting between $\mathbf{J_1}$ and $\mathbf{J_2}$ consists of three segments. The stiffness, or **K** value, of each segment is determined by Eq. 5 and this process is repeated for each spring in the train. In segments with a flexible coupling the total stiffness will be less than the stiffness of the coupling alone. Since the shaft diameters near couplings are the smallest in the machine, their torsional stiffness is fairly low and must be included to avoid large errors. The technique for adding shaft stiffness values is illustrated in figure 6. The equivalent stiffness, $\mathbf{K_E}$, is an inverse sum of the individual stiffnesses as shown in Eq. 6. This procedure works for any number of segments.

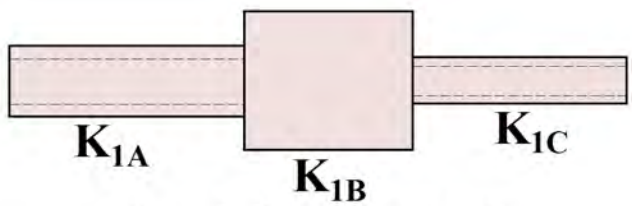

Figure 6 - Multi-Segment Shafting

$$\frac{1}{K_E} = \frac{1}{K_{1A}} + \frac{1}{K_{1B}} + \frac{1}{K_{1C}} \quad \frac{\text{IN-LB}}{\text{RAD}} \qquad \text{Eq. 6}$$

Simple 2-Mass Example: An example of the most basic torsional system is figure 7. The dimensions are given in inches. For this case, the inertia of the shaft segments between the large inertias $\mathbf{J_1}$ and $\mathbf{J_2}$ are ignored. Using Eq. 1, the inertia of $\mathbf{J_1}$ is 27,654 LB-IN^{2}and $\mathbf{J_2}$ is 40,008 LB-IN^2. The total inertia of the connecting segments is ***two orders*** of magnitude below $\mathbf{J_1}$ or $\mathbf{J_2}$ so ignoring these inertias is a valid assumption. Assuming steel as the material, the stiffness of segment $\mathbf{K_1}$ is 24.3 X 10^6 IN-LB/RAD, $\mathbf{K_2}$ is 7.21 X 10^6 IN-LB/RAD, and $\mathbf{K_3}$ is 71.2 X 10^6 IN-LB/RAD. Added up using Eq. 5, $\mathbf{K_E}$, the net equivalent stiffness is 5.16 X 10^6 IN-LB/RAD.

Calculating Torsional Frequencies: There are always $\mathbf{J_N}$**-1** important torsional resonances. A 2-mass system only has one torsional resonance. A 3-mass system has two torsional resonances and so forth. Since we now know how to calculate the necessary inertia and stiffness values, the actual torsional resonance frequencies can be calculated. For the simple 2-mass system the equation, Eq. 7, is not complex.

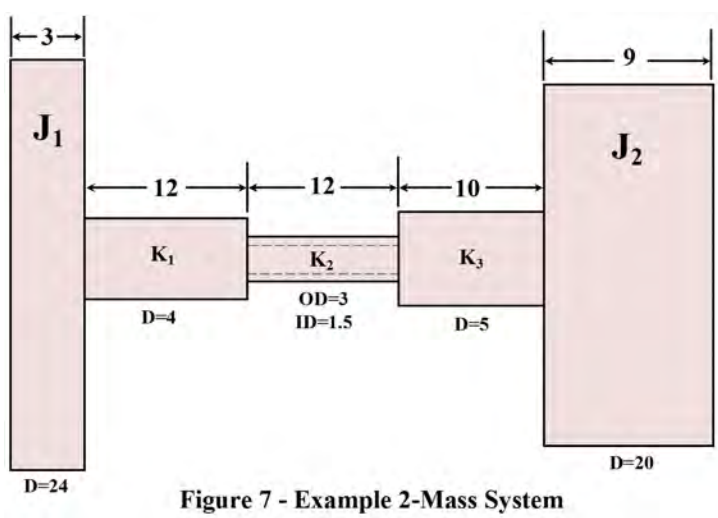

Figure 7 - Example 2-Mass System

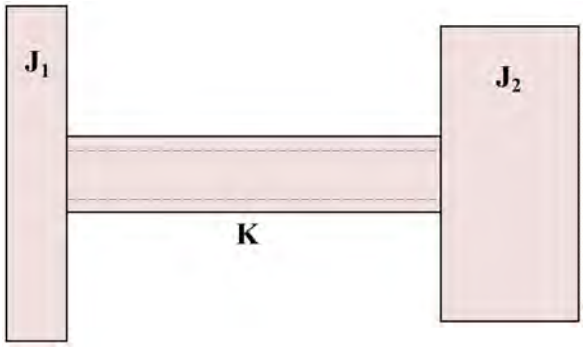

$$\omega_n = \sqrt{K \frac{J_1 + J_2}{J_1 \; J_2}} \quad \frac{RAD}{SEC} \qquad \text{Eq. 7}$$

Figure 8 - Simple 2-Mass System

In order to use Eq. 7, the English stiffness units are IN-LB/RAD and the inertia units are LB-IN-SEC^2. Previously, calculations for the example in figure 7, using Eq. 1, resulted in inertia values with the units of LB-IN^2. To convert these to LB-IN-SEC^2, just divide by 386.088, the appropriate gravitational constant. Thus, the torsional natural frequency of our example system is:

$$\omega_n = \sqrt{5.16 \; X \; 10^6 \left(\frac{71.63 + 103.62}{71.63 \quad 103.62} \right)} = 349 \; \frac{RAD}{SEC} = 3{,}333 \; CPM$$

Unfortunately, the simplicity ends with the 2-mass system. For three masses and two springs, the solution becomes a fourth-order, difficult to solve manually, equation:

$$\omega^4 \left(J_1 \, J_2 \, J_3 \right) + \omega^2 \left[K_2 \, J_1 \left(J_2 + J_3 \right) + K_1 \, J_3 \left(J_1 + J_2 \right) \right] - K_1 \, K_2 \left(J_1 + J_2 + J_3 \right) = 0$$

Geared Systems: Many rotating equipment trains include speed reducing or speed increasing gear sets. In order to calculate the torsional resonance frequencies of a geared train, the stiffnesses and inertias at one of the train speeds must be converted or ***reflected*** to the other train speed by the speed ratio squared. Figure 9 shows a typical geared system. $\mathbf{N_1}$ is the speed at $\mathbf{J_1}$ and $\mathbf{J_2}$ while $\mathbf{N_2}$ is the rotor speed at $\mathbf{J_3}$ and $\mathbf{J_4}$.

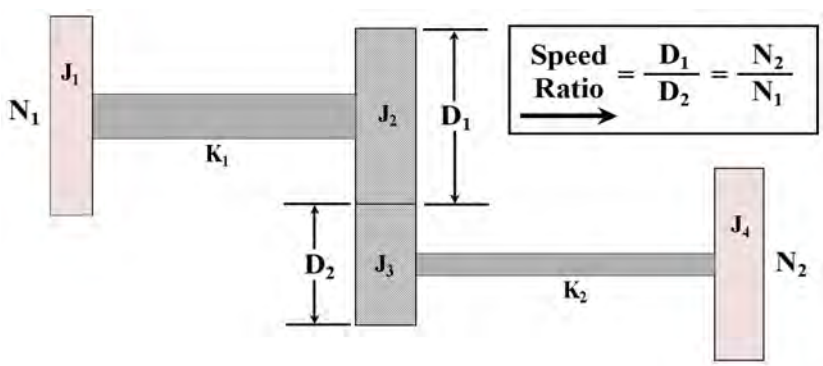

Figure 9 - Typical Geared Torsional System

It does not matter which speed is used as the reference speed. Conceptually, turning the pinion side of a speed reducer gives one a mechanical advantage and the effective low speed side stiffness and inertia seem to be reduced. When turning the low-speed bull gear, it is much more difficult to accelerate the rotor on the high speed side so the apparent stiffness and inertia seem to be greater. Figure 10 illustrates this process.

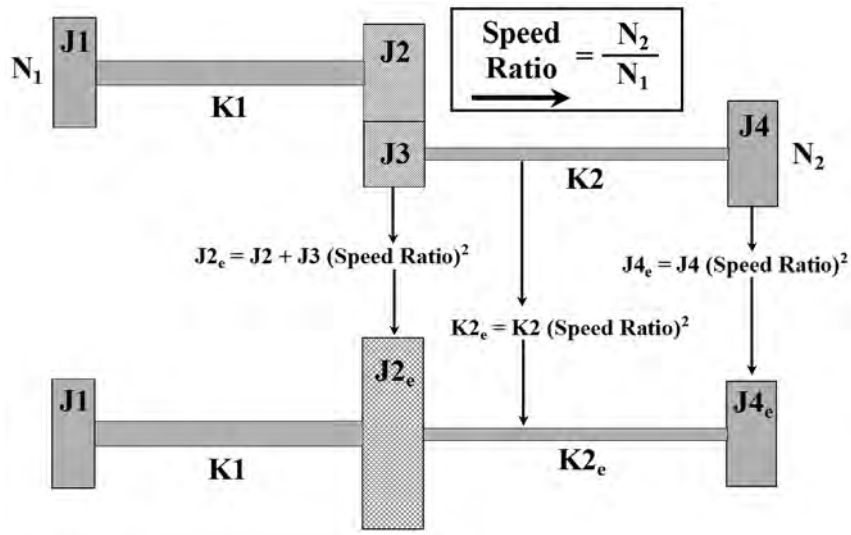

Figure 10 - Reducing Geared System to Equivalent System

For systems with multiple gear sets, this process cascades through the train with a speed ratio squared factor applied sequentially for each gear pair. Torque is altered by the speed ratio directly, not speed squared.

Torsional Mode Shapes: For every torsional resonance frequency (called *eigenvalues*) in a machine train there is an associated torsional resonance mode shape (called *eigenvectors*). Torsional mode shapes are different than lateral mode shapes and require a different perspective. Torsional mode shapes are presented as non-dimensional relative twist amplitude with a maximum of +1 and a minimum of -1. Actual twist amplitudes and shaft stresses can only be calculated from a forced response analysis with a defined forcing function. For the simple 2-mass system, the resonant torsional twist amplitude at the inertia, $\mathbf{J_1}$, will be greater by the ratio of $\mathbf{J_2/J_1}$ with a single node point between the masses. Figure 11 is the calculated ***animated*** mode shape for the example from the figure 7 example.

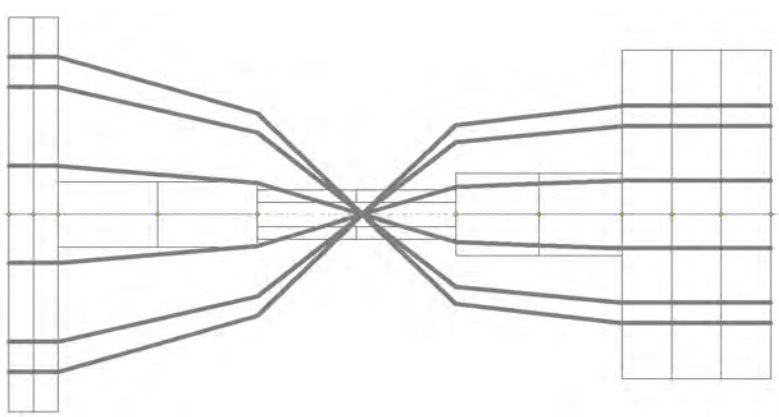

Figure 11- Animated Mode Shape for Simple 2-Mass Example

An animated mode shape shows several cycles of the relative twist amplitude across the equipment train superimposed over the physical outline of the train. In this case the maximum twist amplitude is on the left-land side with the smaller inertia. The smallest inertia has less resistance to oscillatory forces and is more easily rotationally displaced. There is a node point near the center of the weakest connecting link between the two inertias. The slope of the mode shape line indicates the degree of twist in the corresponding segment. The shear stresses are greatest in the shaft section with the greatest mode shape slope. Here the shear stress at the torsional resonance will be a maximum in the middle tube section. The sections next to the center tube have a slight slope with less twist. The sections on the end have no slope to the mode shape line. This means that these sections are acting like rigid bodies or pure lumped inertias. When attempting to measure the torsional resonance, strain gages would produce the maximum output when placed on the most highly stressed part. However, many of the other test methods that measure torsional amplitude will be most responsive at the places where the twist amplitude is a maximum. The testing methods are covered below.

Interference Diagrams: There are often multiple torsional resonances and multiple torsional excitation sources. In order to evaluate these potential interferences, a special *interference diagram* has been developed to show the whole picture at once. Often mislabeled as other types of charts, the interference diagram may be shown in linear format or logarithmic format. The logarithmic format has several advantages including increased clarity and is often more easily understood. Figure 12 is a typical interference diagram with all system frequencies on the horizontal axis and all torsional resonances on the vertical axis. While 2X line frequency is shown here as a potential excitation mechanism, this analyst has never seen a documented case of line frequencies causing significant torsional excitation.

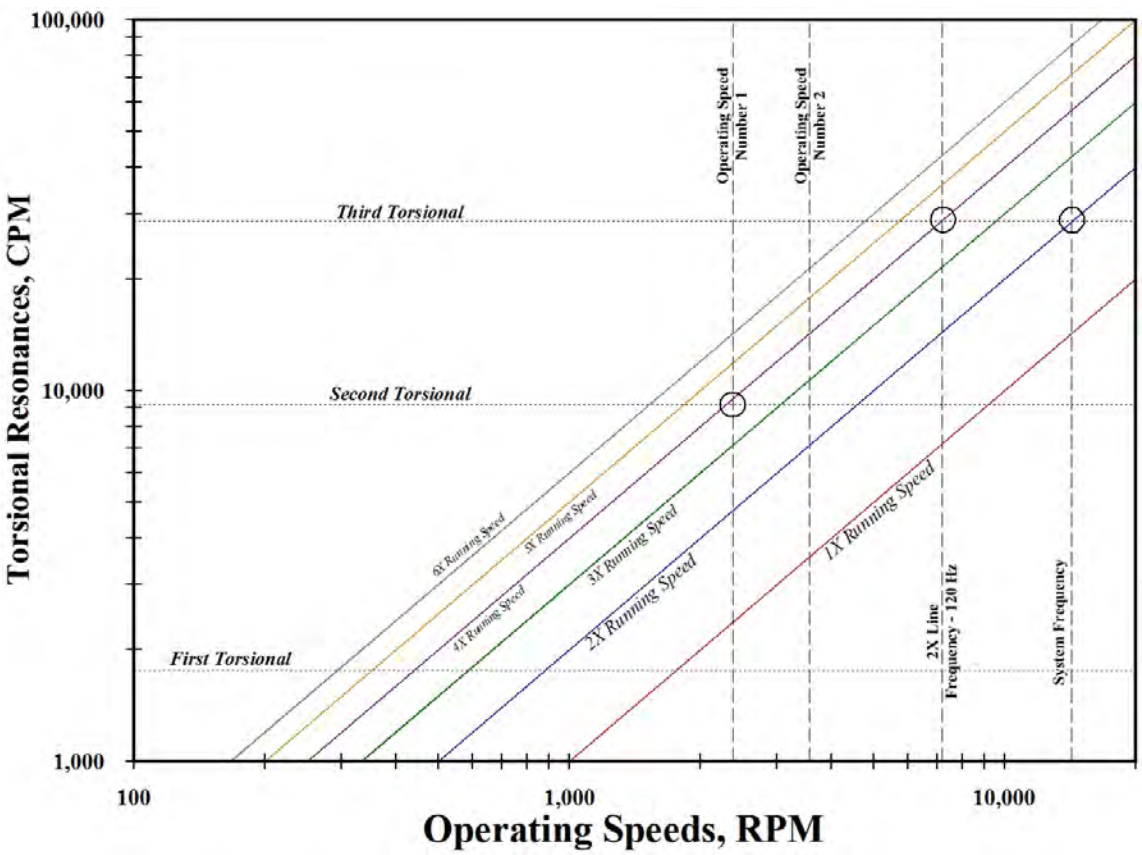

Figure 12 - Typical Torsional Interference Diagram

Forced Response of Torsional Vibration: Forced response analysis has two subcategories: steady state excitation and transient excitation. Steady state forced response usually means constant speed with one or more components in the system producing constant torque pulsations. Transient torsional excitation is produced by changing conditions like speed or load or electrical interruption. Basically, to analyze the transient torsional response of a train, the forces as a function of speed or time must be defined. While it is usually a design goal to avoid torsional resonances, there are systems where torsional resonances will be encountered during normal operation. In these cases a torsional analysis is performed that will predict the probable shaft stress levels. Then the designer can allow for these stresses when selecting shaft sizes and materials. Some of the most common torsional excitation mechanisms:

1. Synchronous motors This is a transient condition encountered only during startup. All synchronous motors produce torque pulsations between start and synchronous speed. These pulsations start at twice line frequency (120 Hz or 100 Hz) and decay to zero Hz when the motor synchronizes. Thus, all torsional resonances between 0 and 7,200 CPM will be excited every time the motor is energized. These torque pulsations can be several times the rated full-load torque of the motor and have been known to cause spectacular machinery failures. The only real source of information about the nature of motor torques is the motor manufacturer. Fortunately, the number of high stress cycles is limited during each start and it is usually possible to design the system components to be strong enough to withstand a reasonable number of start events. An example of a synchronous motor train analysis is detailed below.

2. Reciprocating engines, compressors and pumps This type of machine, whether a driver or a driven produces unsteady torque flow in the system. In an internal combustion engine each time a cylinder "fires" a pressure pulse pushes down on the piston which turns the crankshaft. Reference 1 devotes significant space to the complexities of this type of driver. For the torsional analyst to model a system with a reciprocating machinery component, besides the internal geometry, the magnitude of the pulsations must be defined as well as the firing sequence in a multi-cylinder device and the phasing between pulsations. Getting a complete set of pulsation data information for a machine is not easy as many manufacturers think it is "proprietary".

3. Variable frequency drives In the early days of VFD motors a fairly crude 6-step synthesized power waveform was fed to the motor as a stepped square wave. This produced numerous torque harmonics and caused high vibrations and shaft failures. More modern VFD drive technology like pulse-width modulation has reduced this problem. Usually the drive manufacturer will supply the analyst with a list of torque harmonics with amplitude and phase information.

4. Gears Gear sets change the train speed (except for 1:1 gear ratios) and rotation direction. Gears also take pure rotary torque and produce a lateral and a tangential torque component. The lateral component creates high steady radial loads on the bearings supporting the gears. Any alternating torques will induce alternating radial load and measurable lateral vibration. Thus, the only place in most machine trains that torsional vibration will manifest itself is on the gears. Gears themselves can cause unsteady torque transmission due to accuracy errors in the gear manufacturing process. Some of the conditions that can cause gears to act as a torsional exciter are pitch-line runout, tooth-spacing errors, excessive backlash, low quality gears, and worn gears. The backlash phenomena adds a non-linear element to the analysis that is rarely included. Typically the excitation frequencies associated with gears are at running speed and twice running speed. Higher harmonics are possible but rarely encountered. The user's best defense against having gear torsional problems is to buy the highest quality gears. Gears bought in accordance with the current API 613 specifications typically produce torque pulsations less than one percent of the load torque. Gear mesh frequencies sometimes can act as a torsional excitation mechanism but this is rare. Gears also add an additional torsional stiffness spring that is usually ignored. However in some instances it can be very important. One general equation for the stiffness of spur gears is given in Eq. 8.

$$K_T = 1.6 \; X \; 10^6 \; (Face\ Width)\ (Larger\ \ Gear\ \ Pitch\ \ Radius)^2 \qquad \text{Eq. 8}$$

5. Sudden load changes Every time an electric motor is energized, a torque shock is generated that will "ring" the torsional resonances of any machine train. Fortunately the duration of the resulting oscillations is short and does not normally cause any harm. On complex systems, very high stress levels have been measured and caused the use of a "soft-start" system that applied initial torque gradually. Sudden load removal is also a torque pulse and occurs every time a motor is turned off or a turbine trips. These events do not generally cause excessive torsional oscillations. One of the worst type of situations is a total load shed on a large multi-megawatt turbine generator train similar to figure 13. This train is nearly 100 feet long and the rotating mass is over 235 tons. Since this train is so long and has so many torsional modes the transient stresses can be enough to damage or break a shaft or the long low pressure turbine blades.

Figure 13 - 800 MW Steam Turbine Generator Train

6. Electrical system interaction This is a complex subject since it involves coupling the mechanical system to the electrical grid. This is very important in large turbine-generator sets and is discussed in reference 2. Normally a mechanical equivalent system to the electrical grid is constructed with analogs for stiffness, damping and inertia. Electrical faults such as short circuits can induce extreme torsional excitations. Bad contactors and switches have also been known to excite torsional resonances. There is also speculation that line frequency and twice line frequency can act as a torsional exciter. However this author has never seen this nor been able to find a single documented case of line frequency interaction not associated with a mechanical or electrical fault.

7. Lobe-Pass, blade-pass, and vane-pass frequencies Torque pulses can be generated each time a blade in an impeller passes a stationary object or there is non-uniform flow or off-design operation. The worst case would be a surge that generates very large impulse forces. In positive displacement machines like screw compressors, 2 to 3 percent of the load torque can be produced at the lobe-pass frequency.

8. Couplings Universal joints or "Hooke's joint" couplings produce significant torsional pulses at twice rotational speed that increase in amplitude as the offset between the shafts increase. Sometimes a torsional resonance can be tamed by simply reducing this offset. Other coupling types can also produce 2X torque oscillations when there is misalignment between shafts, but these are generally low in amplitude.

Torsional Damping: It is well known that torsional damping is very small in most rotating equipment trains. There are two types of torsional damping. Discrete damping occurs at individual points and is extremely difficult to quantify. Modal damping is a system property and has different values for each torsional resonance. Some examples of discrete damping are the attached electrical system, fluid film bearings (mostly in gear sets), frictional slippage and so-called "damper" couplings. Damper couplings have an elastomer as part of the torque path. In reality, it is not the damping that allows these devices to attenuate torsional vibration, it is the non-linear nature of the elastomer spring rate and damping rate. These are also frequency dependent. As torsional oscillation amplitude increases, the elastomer torsional stiffness increases. This changes the torsional resonance, lowering the amplitude. Essentially the elastomeric coupling makes the torsional resonance a moving target. Gear type and grid type couplings also add small amounts of torsional damping. The down side is that, in acting as a damping mechanism, wear occurs and these parts will need regular lubrication and maintenance. There are also some viscous or fluid coupling devices that add discrete damping and also are very soft torsionally. Damping dissipates resonant energy into heat. If a "damper" of any kind is used to purely attenuate torsional amplitude at a constant speed, there must be provisions for removing the heat generated.

Modal damping is the technique most often when analyzing torsional forced response of rotating equipment trains. It is a percentage of critical damping for each torsional mode. The actual modal damping is very difficult to measure and is assumed to be 1 to 3 percent in most cases, however it can be as low as 0.2 percent or as high as 7 percent depending on the system. This is often a judgement call by the analyst. Some of the sources of modal damping are material hysteresis and working fluid interaction.

Shaft Stress and Fatigue: The torsional stress, **PSI**, in a solid circular shaft is $\mathbf{16T/\pi D^3}$ where **D** is the outside diameter in inches and **T** is the torque in inch-pounds. Depending on the material and the service and environmental factors, machinery designers select shaft sizes based on an assumed endurance limit. The endurance limit is that stress level at which (theoretically) an infinite number of cycles is possible without failure. In reality there are too many variables to set an exact endurance limit. For this reason, guidelines are often given for particular situations. Stress concentration factors must also be included when setting the acceptable stress value for any system. In the aircraft industry where weight is a major consideration, the acceptable stress limit often exceeds 20,000 PSI for shafting. In the petrochemical industry it is fairly rare to find torsional stresses exceeding 15,000 PSI and in severe duty or if corrosion is a factor, the stress is limited to less than 10,000 PSI. All fatigue cycles are cumulative and build up over the life of the component. Low cycle fatigue occurs when the stress is high enough to cause plastic deformation. High cycle fatigue involves the accumulation of elastic deformations. Figure 14 is an actual **S-N** plot for a typical shafting material. Here the plot is for bending stress. In practice the net shaft stresses are the vector sum of torsional and lateral bending stresses.

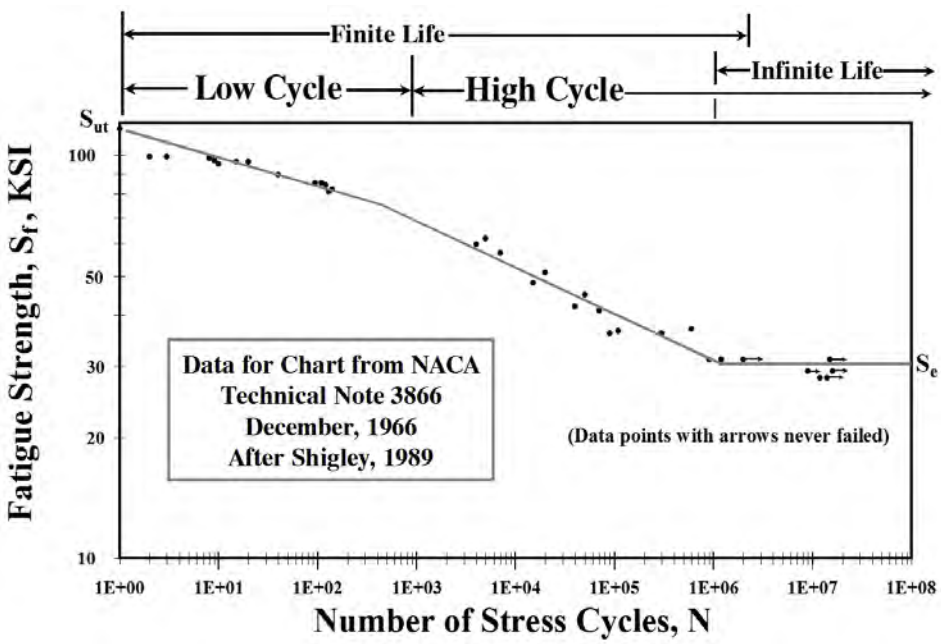

Figure 14 - Typical Fatigue-Stress Cycle Plot for Steel

When shafting fails due to fatigue from oscillatory torsional stresses there is a characteristic 45 degree break. This is the weakest plane in torque shear. Quite often the fatigue failure starts in a keyway, sharp corner, or other stress riser point. Good machine design practices try to minimize stress risers and lower stress concentration factors. The forced response analysis attempts to predict the torsional stresses throughout the train during transient events like a synchronous motor start or at a steady speed. Many of the cited references cover this topic in detail.

Example Analyses: Four examples are presented. All are based on actual industrial installations where unusual vibrations or failures were not solved by the typical route of balancing, alignment and operational adjustment. In many cases the problems lingered for many years before the torsional analysis revealed the underlying cause of the problems. The simplest type of torsional system is a driver and a driven like a turbine driving a fan or a motor driving a pump through a flexible coupling. The severity of any torsional problem is determined by the effect a torsional resonance is having on operational availability and maintenance.

The simple 2-mass system illustrated in example 1 is an induction motor driving a centrifugal pump as indicated in figure 15. This is a typical API type process pump in light hydrocarbon service. The operating speed is 1,775 RPM and impeller has 3 vanes. Pressure pulsations from the impeller occur at 3X or 5,325 CPM.

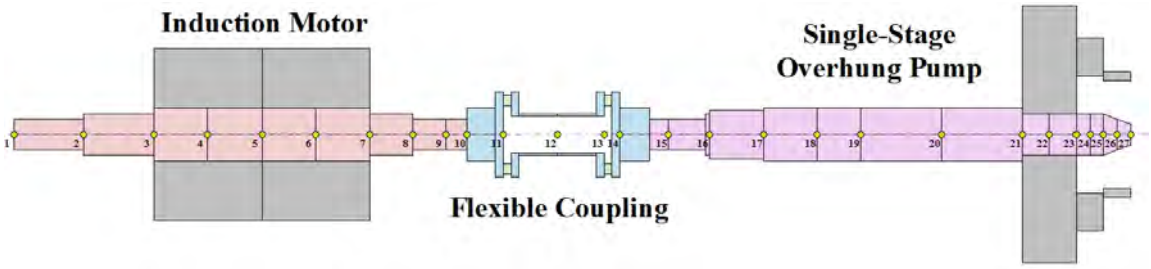

Figure 15 - Example 1 - Simple 2-Mass Torsional Motor-Pump Train

High vibrations on this train were detected at vane-pass frequency. Modifications to the pump including the "A" and "B" gaps and piping had little effect on reducing the 3X vibrations. A torsional analysis indicated that the first torsional resonance was 5,300 CPM. It was not possible to increase or decrease the coupling torsional stiffness enough to move the torsional resonance more than 100 CPM. The solution was to purchase a new impeller with 4 vanes moving the pressure pulsations well above the torsional resonance. The modified train ran smoothly after the impeller change and the seal and bearing failures were significantly reduced.

A basic geared system is illustrated by the turbine driven induced-draft fan train shown in figure 16. This train exhibited severe gear wear causing the gears to be replaced every 14 to 18 months. Many "fixes" were implemented including precision component balancing and hot alignment. These efforts did not decrease the failure rate. Finally, based on the gear manufacturer's recommendation, a torsional analysis was conducted after it was found that the original design effort had ignored this aspect.

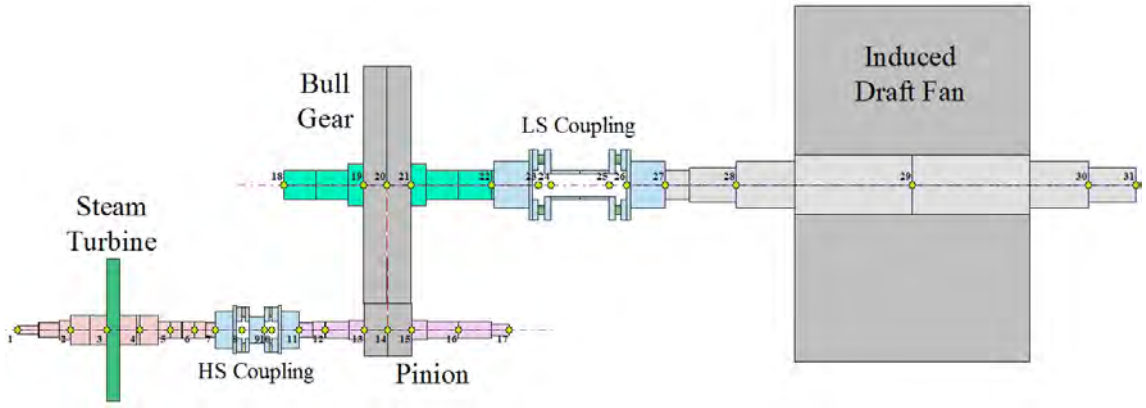

Figure 16 - Example 2 - Turbine Driven Induced Draft Fan Train

The gear ratio for this train was a 5.97:1 speed decrease. The torsional analysis revealed an unusual problem. The first torsional resonance was found to be coincident with the fan speed (750 to 770 RPM) and the second torsional resonance was found to be at the turbine speed of 4,480 to 4,600 RPM. The couplings were examined for possible modification and it was determined that stiffening the couplings would have no significant influence on the torsional resonances. Instead, the torsional stiffness of each coupling was reduced to give the necessary separation margin. Table 1 is a summary of the findings.

Coupling Stiffness IN-LB/RAD	1st Torsional Resonance (CPM) Separation Margin (%)	2nd Torsional Resonance (CPM) Separation Margin (%)
Original L.S. 75.2 X 10^6 H.S. 16.6 X 10^6	760 CPM (None)	4,540 CPM (None)
Modified L.S. 33.1 X 10^6 H.S. 5.02 X 10^6	647 CPM (12.6%)	3,872 CPM (12.4%)

Table 1 - Summary for Example 2 - Turbine-Gear-Fan Torsional Resonances

Once both couplings were replaced the system vibration dropped from near 0.5 IPS to less than 0.1 IPS and there has been no significant gear deterioration for over five years.

One of the most severe examples of transient torsional excitation occurs during the start of a synchronous motor. Example 3 (figure 17) consists of a 6-pole 5,500 HP synchronous motor driving an air compressor through a gear speed increaser. In this case torsional problems were eliminated in the design stage.

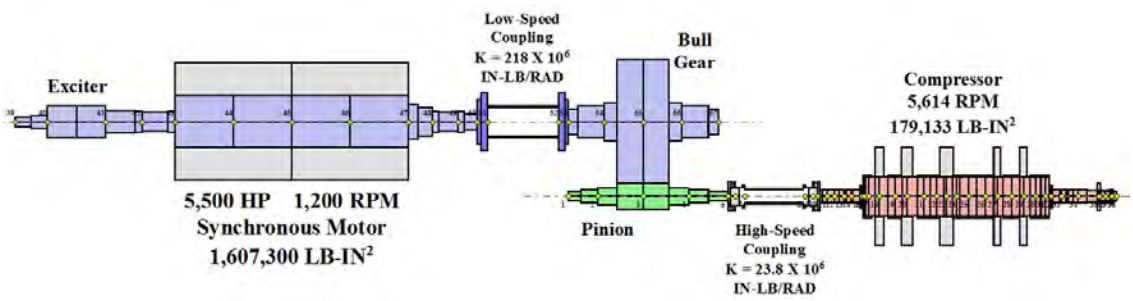

Figure 17 - Example 3 - Synchronous Motor-Gear-Compressor Train

Every synchronous motor generates alternating torque impulses during a startup. These pulse begin at twice line frequency (7,200 CPM in the US) and decline inversely with speed to zero when synchronous speed is attained. This means that every torsional resonance between 0 and 7,200 CPM will be excited during each startup. These torque pulsations are not trivial and have been the cause of many machinery failures. Thus, any machine train with a synchronous motor must be evaluated with a transient torsional analysis. A transient analysis consists of creating a spring-mass model and defining all the torque producers and absorbers. The torque information is generally available only from the motor vendor who must communicate with the manufacturer of the other machinery and produce a set of torque curves similar to figure 18. A forced response procedure is applied to the model simulating the startup. At time zero, the driving, oscillatory, and load torques are applied simultaneously. This causes the train to accelerate in speed. Then, at very small time steps, a new speed is calculated along with the torsional oscillation amplitude. Ultimately, the alternating torque amplitudes are converted to the shear stresses in the shafts. One important calculation coming from this analysis is the time to reach full speed as seen in figure 19. Anything over 20 seconds could be damaging to the motor. After synchronization, the motor torque is balanced by the load torque and there are no more alternating torque pulsations from the motor. Very low frequency oscillations often seen immediately after synchronization are due to interaction of the mechanical system with the electrical grid.

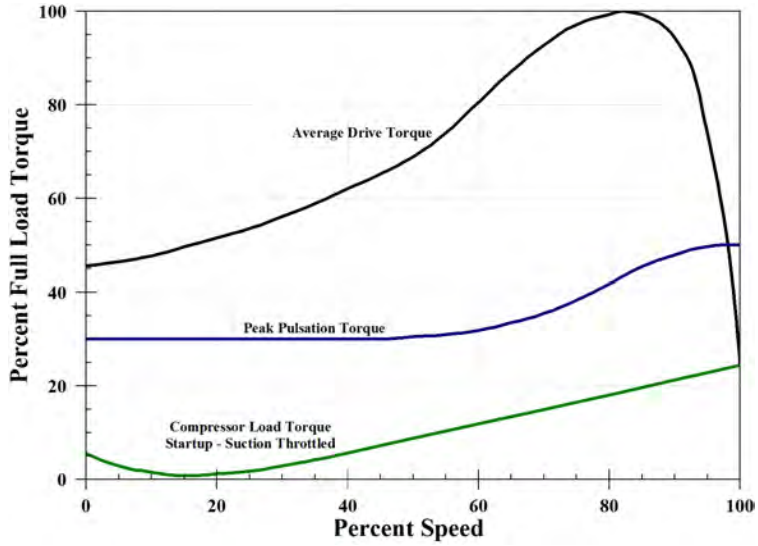

Figure 18 - Speed vs. Torque Curves for 5,500 HP Synchronous Motor

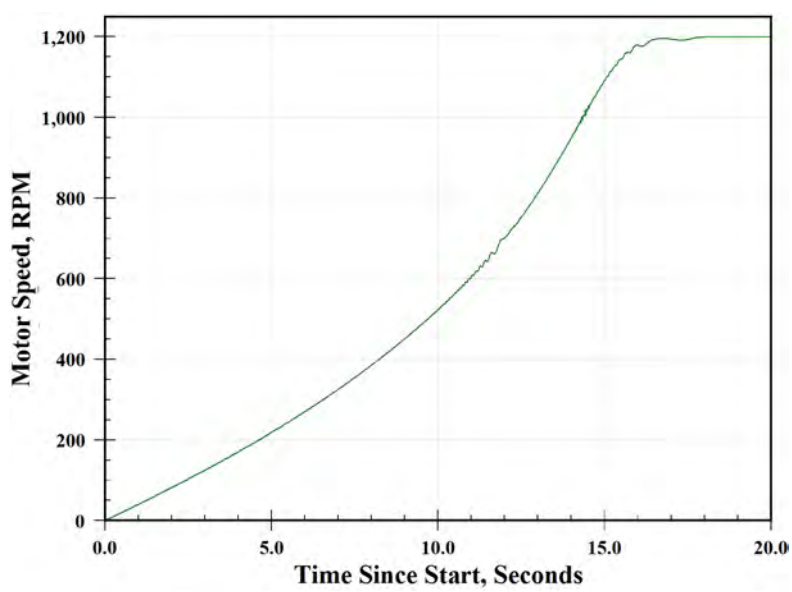

Figure 19 - Startup Time Calculation for Synchronous Motor-Gear-Compressor Train

Ripples in the time-speed curve of figure 19 are actual speed fluctuations due to the torsional resonances. The first resonance encountered 11.8 seconds into the startup is the second torsional resonance at 3,260 CPM. The first torsional resonance, at 1,275 CPM, is encountered at 14.5 seconds into the startup. Figure 20 is the animated mode shape of the first torsional resonance. All of the twist amplitude is between the motor and the bull gear. This is where the maximum shear stresses will occur. For this reason the coupling flanges on both the motor and the bull gear were made integral with the shafts. This avoids any stresses associated with shrunk-on hubs or keyways. Figure 21 shows the second animated torsional mode shape. Here there is twist across both couplings. In both these figures, for visual enhancement, the relative twist amplitude is referenced to the compressor speed. The low speed twist amplitudes are actually reduced by the gear ratio value. Figure 22 is a plot of the alternating shaft shear stresses in the motor during a portion of the startup. Figure 23 shows the maximum high speed shaft shear stresses same time period.

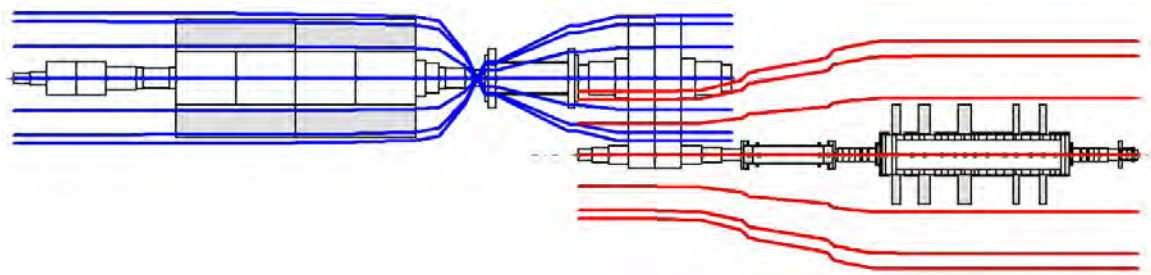

Figure 20 - First Torsional Resonance Mode Shape for Example 3 - 1,275 CPM

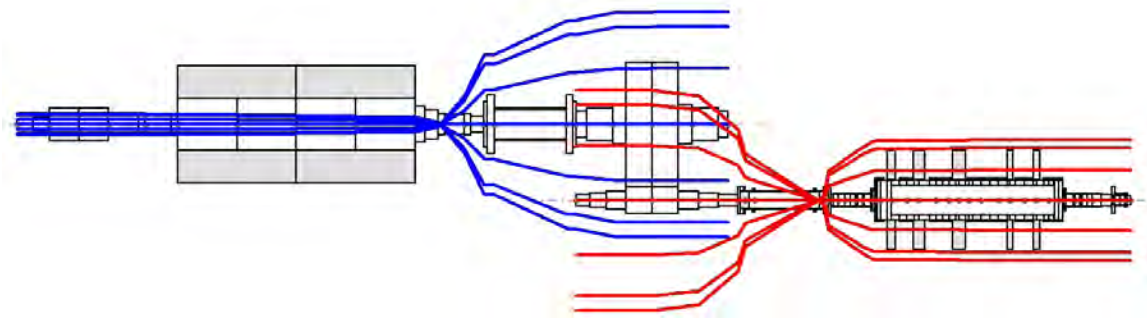

Figure 21 - Second Torsional Resonance Mode Shape for Example 3 - 3,260 CPM

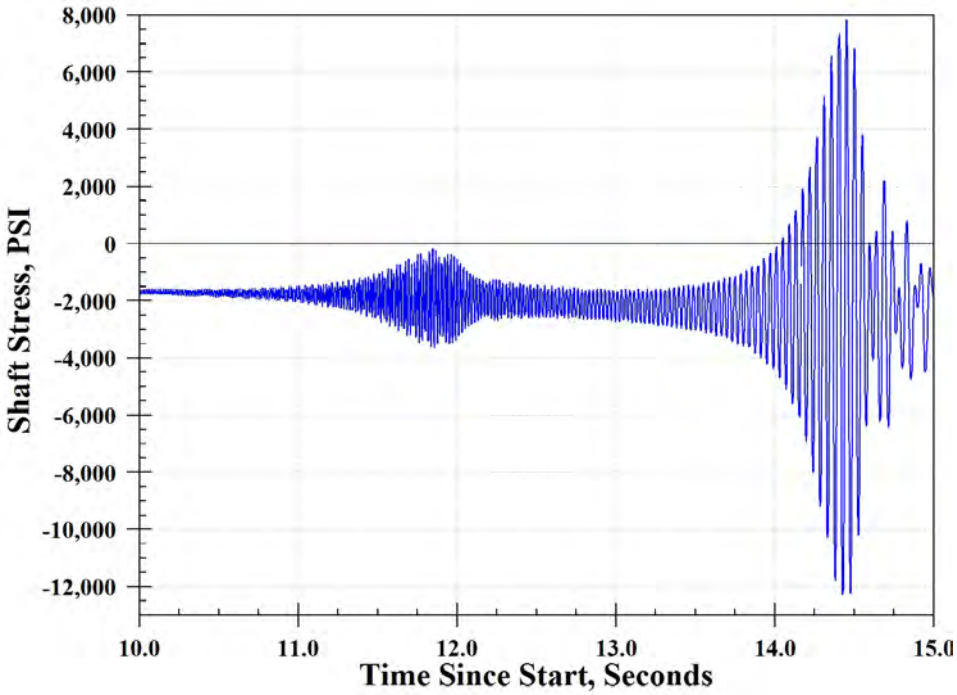

Figure 22 - Maximum Low Speed Shaft Stresses During Example 3 Startup

Due to the presence of driving torque, figure 22 shows the shear stresses offset below zero by the amount of the steady torque. The second torsional resonance reaches a maximum of 1,400 PSI, peak at about 11.8 seconds. The first torsional resonance with 10,000 PSI, peak is much more severe around 14.5 seconds.

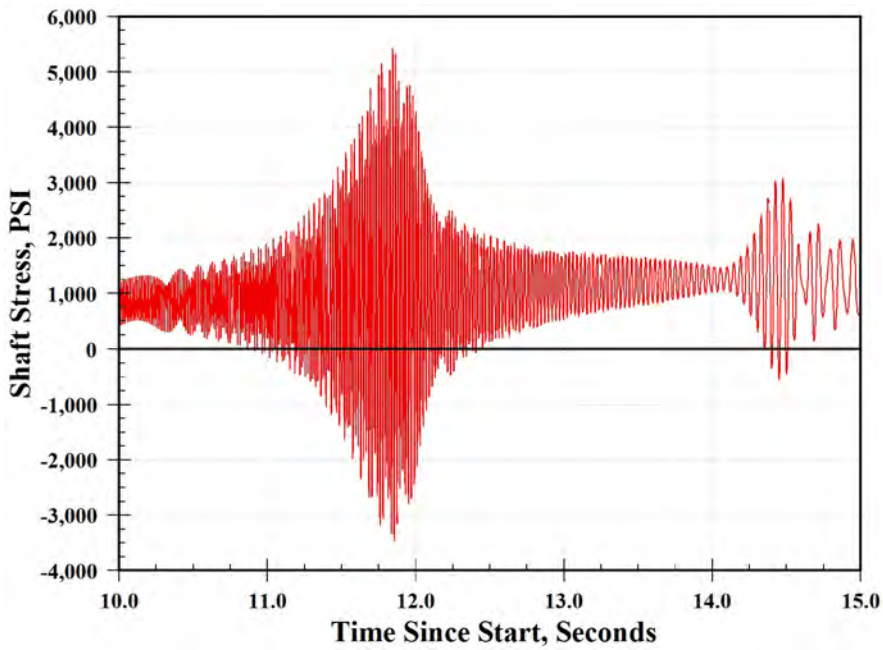

Figure 23 - Maximum High Speed Shaft Stresses During Example 3 Startup

Figure 23 is similar but with the second torsional resonance producing 4,500 PSI, peak shear stress and the first torsional resonance only 1,800 PSI, peak shear stress. This is because there is little relative twist in the high speed shafting during passage through the first torsional resonance. These plots clearly show the decreasing frequency of the torque pulsations.

It is possible to use these plots to determine the number of shear stress cycles that will accumulate and potentially fatigue the shaft as indicated in figure 14. There are a number of techniques for doing this which are beyond the scope of this paper but are detailed in several of the references. The ultimate goal is infinite life but it is not unusual to settle for a finite life as long as it is economically feasible. Example 3 is a case where good design practices resulted in a machine train with an estimated 2,000 startups before a failure would occur. This train (as documented in reference 6) ran extremely smoothly for 15 years before being retired for a larger capacity unit. It is a credit to the designers that there were no problems throughout the life of the train even though the first torsional resonance at 1,275 CPM was less than 7 percent away from the 1,200 RPM operating speed.

The fourth example involves an engine driven triplex positive displacement pump. This train is mounted on a truck and is used in the oil production industry to force large amounts of nitrogen into the earth to drive out crude oil. One pump can empty a large tank of liquid nitrogen in about 10 minutes. Figure 24 is a photograph of the truck and tank and the triplex pump. These units are in relatively severe duty and had a history of vibration and component failures. Extensive testing, covered below, revealed a torsional resonance associated with twice pump speed and three times pump speed. The 2X forcing function is generated by the universal joint driveshafts and the pump delivers 3X torque pulsations. Figure 25 is the computer model created to analyze this train. This model was simplified due to lack of specific engine, transmission, and transfer case details. The pump operating speed range is 500 to 850 RPM. The “normal” speed is 680 RPM but there are few limitations imposed on actual operation. The torsional analysis and testing revealed a train torsional resonance at 1,640 CPM. This resonance will be excited by the 2X at 820 RPM and by the 3X at 547 RPM. Strong reactions from both 2X and 3X excitations were found at up to 2 degrees peak oscillation.

Figure 24 - Truck Mounted Triplex Pump

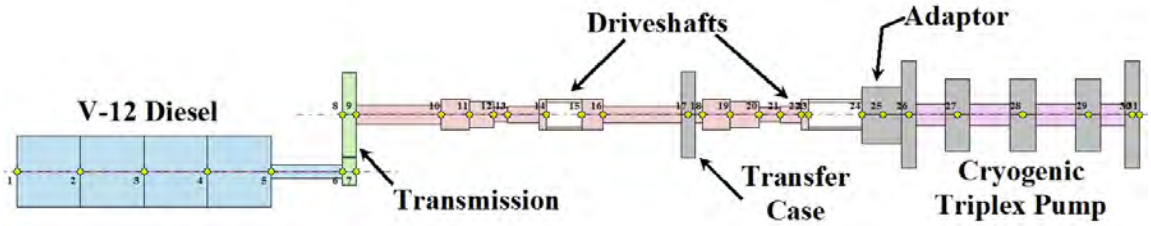

Figure 25 - Computer Model of Engine Driven Triplex Pump

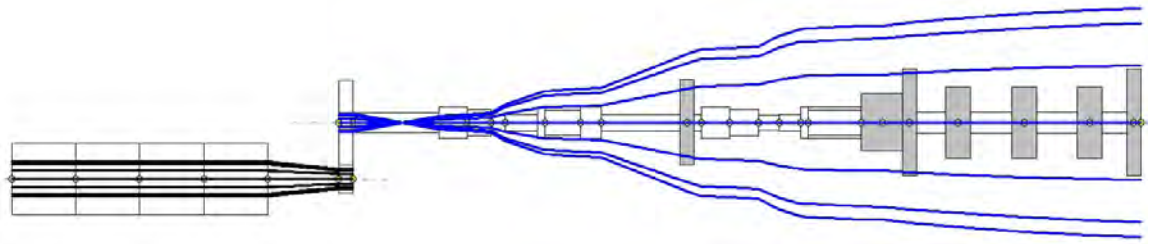

Figure 26 - Torsional Resonance Mode Shape for Example 4

The mode shape, figure 26, indicates the engine and pump are acting as rigid inertias. There were severe restrictions on the type of "fix" that could be applied to this system. First, everything had to fit in the current space. The truck could not be made longer. Stiffening the driveshafts was not possible since making them infinitely rigid would not help. Softening the driveshafts would have compromised their torque carrying capability. Most of the flexibility was in the transmission and transfer cases which could not be modified. Likewise the pump itself was not a candidate for internal change. Since the pump is acting as a rigid lumped inertia with high twist amplitude, adding inertia would lower the resonance. The adaptor between the driveshaft and the pump was increased to as large a diameter as would fit. This added about 30,000 LB-IN^2 to the pump

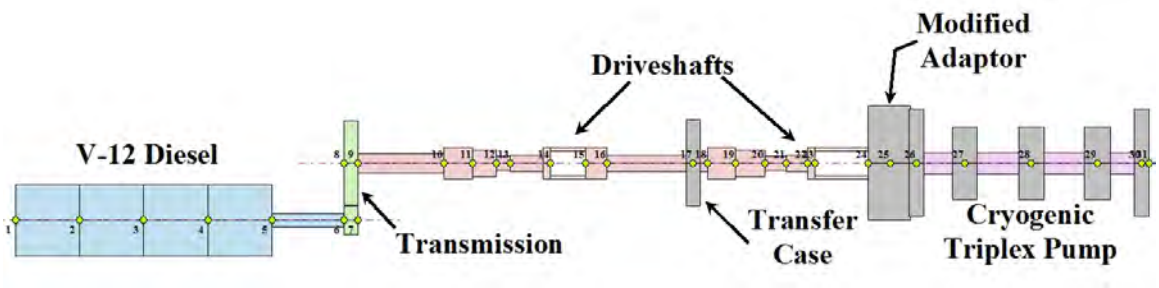

inertia. Figure 27 shows the modified train.

Figure 27 - Triplex Pump Train with Added Inertia

The modified system has a torsional resonance frequency of 1,080 CPM putting the 2X interference at 540 RPM and the 3X resonance at 360 RPM. Operators were cautioned against prolonged operation at these speeds. When the modified adaptor was fitted there was a dramatic decrease in vibration and over time a significant drop in failures. The experimental testing section has more details on this example.

Three of the examples have shown that systems with torsional resonance problems can be modified in several ways. The frequency of the pulsations was altered in example 1 with an impeller design change. Example 2 showed that changing the coupling stiffness is often the easiest way to shift torsional resonances. Example 4 used an inertia change to move torsional resonances away from interfering with operation.

Example 3 is a case where the system had to be designed to withstand known torsional excitations and fatigue cycles. Ideally, all machine trains should be analyzed before a significant amount of money is invested in a design. It is always more expensive to retrofit a system than to have avoided the problem with good design. The same company that builds the triplex pump train recently introduced a 5-cylinder quintiplex pump for delivering ever greater quantities of nitrogen. This time the torsional design was considered from the beginning and the new engine driven pumps are the smoothest ever seen in that industry.

Unit conversion factors: The table provides common unit conversions for torsional analysis.

Multiply	By	To Get
Length, Inches	25.4	Millimeters
Polar Moment of Inertia LB-IN^2	1/386.088	LB-IN-SEC^2
Polar Moment of Inertia LB-IN^2	2.929×10^{-4}	Kg-M^2
Torsional Stiffness IN-LB/RAD	0.11298	N-M/RAD
Weight, LBm	1/386.088	Mass, LB-SEC^2/IN
Weight, LBm	0.45359	Kilograms
Force, LBf	4.4482	Newtons
Power, HP	745.7	Watts
Stress, PSI	6894.8	N/M^2 (Pa)

Selecting a Method for Testing: A well ordered plan must be developed to assure that an effective test method will be used once a need has been identified for measuring torsional response. The previous information describing the typical characteristics for torsional vibration response must be used in establishing an effective method to determine the torsional vibration reaction.

Torsional mode shapes are different for the various torsional vibrational modes that are possibly present. In many cases, there are only one or two modes of interest, with reactions that are well suited to simple measuring methods. However, it is usually not wise to attempt torsional vibration measurement without first performing a torsional analysis as described in the previous sections of this paper.

Torsional vibration in itself is normally not a concern, but the dynamic stresses that result can cause fatigue failures of shafting. Shaft systems that include gears will often have practical limitations on torsional vibration response to prevent the teeth from unloading and transmitting transient reverse torque loading (loading on the backs of gear teeth). However, regardless of the equipment involved, torsional system vibration response can normally be measured more simply than torsional stress.

Review of the torsional mode shape for the simple two-mass system shown in Figure 11 indicates that there is a node point at or near the coupling connecting the two masses when it is excited near the resonance corresponding with the mode shape indicated. If torsional vibration was to be measured, it would be ideal to measure it near the locations of highest torsional response, i.e. at the ends of the shaft (at the masses). If an attempt was made to measure torsional vibration near the coupling connecting the two, the response amplitude would be quite low as indicated by the mode shape.

Torsional vibration would often be recorded at one or more locations in the machine train at accessible locations, followed by review of the torsional mode shape for the mode of interest so that the actual response of the whole machine train can be estimated using the relative amplitudes from the torsional analysis report. Measurement of multiple torsional modes will often require data from more than one shaft location. Figures 20 and 21 show two different mode shapes for a motor gear compressor system. The torsional vibration response for both modes shown could be documented by measuring response at the compressor rotor, or at the bull gear. Measurement at the exciter end of the motor would be quite effective on the 1st mode, but relatively low on the 2nd mode. Attempted measurement of the 2nd torsional mode on the exciter end of the motor will likely produce more uncertainty in the extrapolated mode shape resulting from the relatively low amplitude at the point of measurement.

Alternatively, the system response can also be documented by measuring the shaft torsional shear strain at locations of high relative twist. The torsional shear strain measurement is an indirect measurement of torsional shear stress, which can be used to directly assess the possibility of shaft fatigue. Measurement of torsional shear strain also requires access to the shafting to allow mounting of strain gages and the necessary measurement equipment. The locations where high relative twists (and high shear strain) occur are normally near shaft ends connecting adjacent equipment and on coupling spacers. These locations can also be relatively accessible for strain measurement. Using again the torsional mode shape shown in Figure 11, the most ideal location would be on the smaller diameter shaft section near the anti-node (point of zero crossing on the mode plot), which would be the location of highest mean and alternating shear stress.

Torsional Vibration Measurement: Measurement of torsional vibration is accomplished by using some method of directly measuring the torsional vibration response of the shaft at either a single axial location, or at multiple locations. The methods used for measurement of torsional vibration have varied over the years, with current practice including primarily the use of optical encoders and some sort of torsional demodulation device. However, other methods do exist as described below:

<u>Torsiograph:</u> The torsiograph is a device that is directly connected to a free shaft end such as a gearbox blind end or on the free end of an engine. Torsiographs were made years ago by a number of companies, including hardware variations from purely mechanical devices to a sort of generator device, and some with proximity probes using slip rings to transmit the response to analysis equipment.

One device used in the late 1980's included a torsiograph manufactured by HBM (Hottinger Baldwin). This device was the standard transducer used within the power, refining and chemical industry at that time. It was composed of a rotating flange assembly that would mount directly onto a free shaft end as indicated in API 613[7]. The standard connection detail is shown in Figure 28.

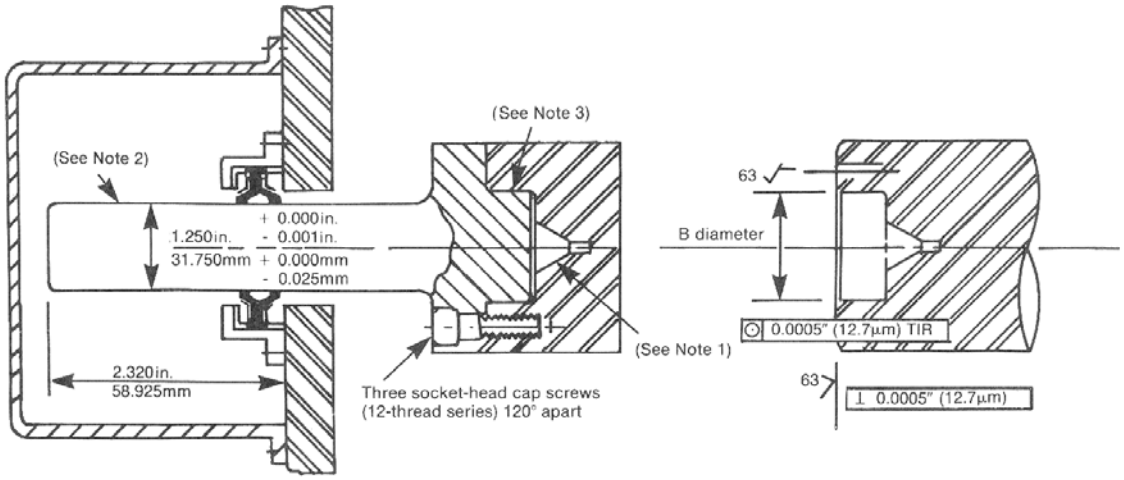

Notes:
1. It is very important that the centering hole for the gear (pinion) shaft be permanent in the counterbore.
2. The stub shaft extension is to be machined true with the journals.
3. The tolerance for the B diameter is to be from 0.000 to 0.001 inch (0.0 to 25.4 micrometers) tight.
4. TIR = total indicated runout.

Figure 28 - Standard Torsiograph Mounting Detail

The torsiograph was to be mounted directly on the shaft end, with torsional vibration transmitted via slip rings to a non-rotating casing. The torsional vibration was generated by displacement probes that would measure the relative motion between an inertial disk that was mounted through torsional springs to the rotating shaft assembly and the rotating shaft.

Several drawbacks exist for using a torsiograph including limits on angular acceleration and inability to transmit low frequency response. The limit on angular acceleration is due to the compression of the torsional springs between the floating inertial disk and the rotating shafting. The limit would be expected to be approximately +/- 3° relative movement between the disk and shaft, producing an angular acceleration limit defined by the torsional stiffness of the springs. The low frequency response limit is caused by the high pass filter characteristics of the spring-mass combination of the inertial disk, and can easily limit useful measurement to 3 Hz or higher.

<u>Demodulation using Proximity Probes:</u> Proximity probes can be used when aimed at a toothed gear to measure the torsional vibration by using a demodulation technique where the relative spacing between gear teeth are used to measure the torsional vibration. The response pattern measured from a gear tooth would be similar to Figure 29.

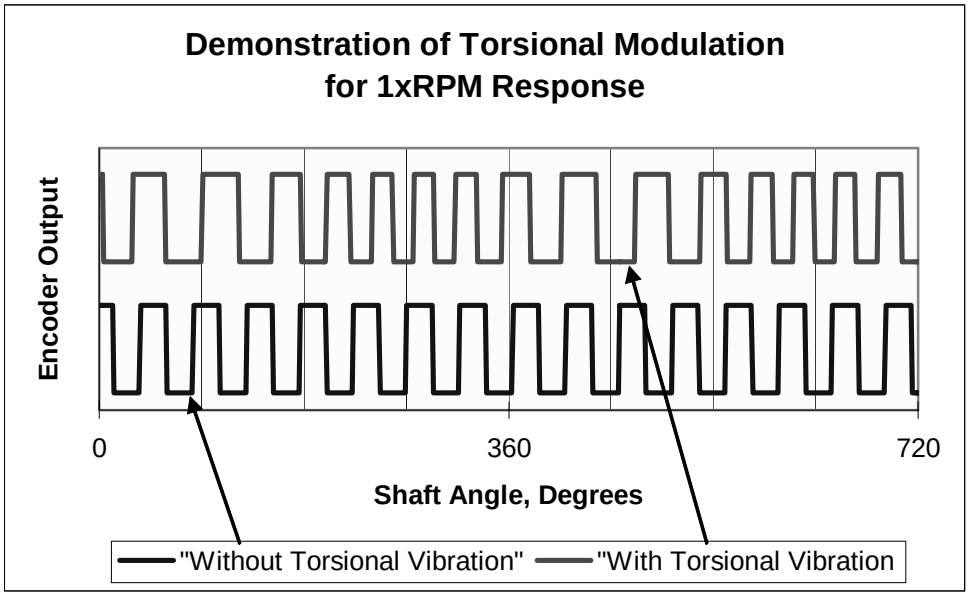

Figure 29 – Signal from Proximity Probe Looking at Gear Tooth

The demodulation device would then be used to determine the relative angular velocity (instantaneous speed) from pulse to pulse and convert that to angular velocity in degrees/second.

Limitations found using proximity probes include measurement difficulties due to variation in the surfaces of the gear teeth the probe is used to look at. These variations can produce significant noise levels that can make the measurement very difficult. Common torsional response amplitudes in turbomachinery applications can be as low as 0.07 degrees zero-to-peak, making the demodulation method using proximity probes challenging.

Optical Encoder Method: Optical encoders are a currently available method with very good accuracy, and when done properly, very low noise. An optical encoder is a rotary device that has a precision optical disk mounted internally that produces a number of very accurate pulses per revolution. A typical encoder is shown in Figure 30.

The generated pulse train is similar to that shown in Figure 29, but will generally have lower noise, and better results for particularly low torsional response amplitudes compared to using proximity probes on gear teeth. One drawback to the encoder is that it too must be mounted on the end of a shaft. However, this obstacle can be overcome by using a measuring wheel. A measuring wheel is a precision rubber coated disk that is mounted to the encoder, allowing the encoder to be coupled to the shaft using the rubber wheel. Use of the measuring wheel will allow one to position an optical encoder at any shaft position where there is about 5” of axial length available.

Typical mounting methods used for loading the encoder measuring wheel against a shaft section are shown in Figures 31 and 32. Great care must be used to assure that the wheel is fitted perpendicular to the shaft axis, and that it will not walk axially along the shaft. The best method to prevent axial travel is to provide an axial restraint on the encoder mount, and to locate the encoder so the mounting arm is always in slight tension (pulling on the arm) opposed to compression. It is also best to rotate the shaft at slow speed to verify that the encoder is contacting the shaft well, and that it will not drift axially prior to full speed operation.

Use of the measuring wheel will generally result in some slippage due to the rubber wheel rolling on the shaft, but the slippage is normally less than several percent of rotation speed. The primary drawback to using the encoder method with the measuring wheel is that any relative vibration between the shaft and the mounting location of the encoder support will produce apparent torsional vibration on the signal output. This can normally be eliminated by mounting two encoders on opposite sides of the shaft and using the

signals from both to evaluate the potential for noise from shaft vibration. Synchronous runout of the shaft surface will produce an apparent torsional vibration response at 1X RPM, but this amplitude can be calculated using TIR measurements and compared to expected torsional vibration amplitudes to determine if the test method is appropriate.

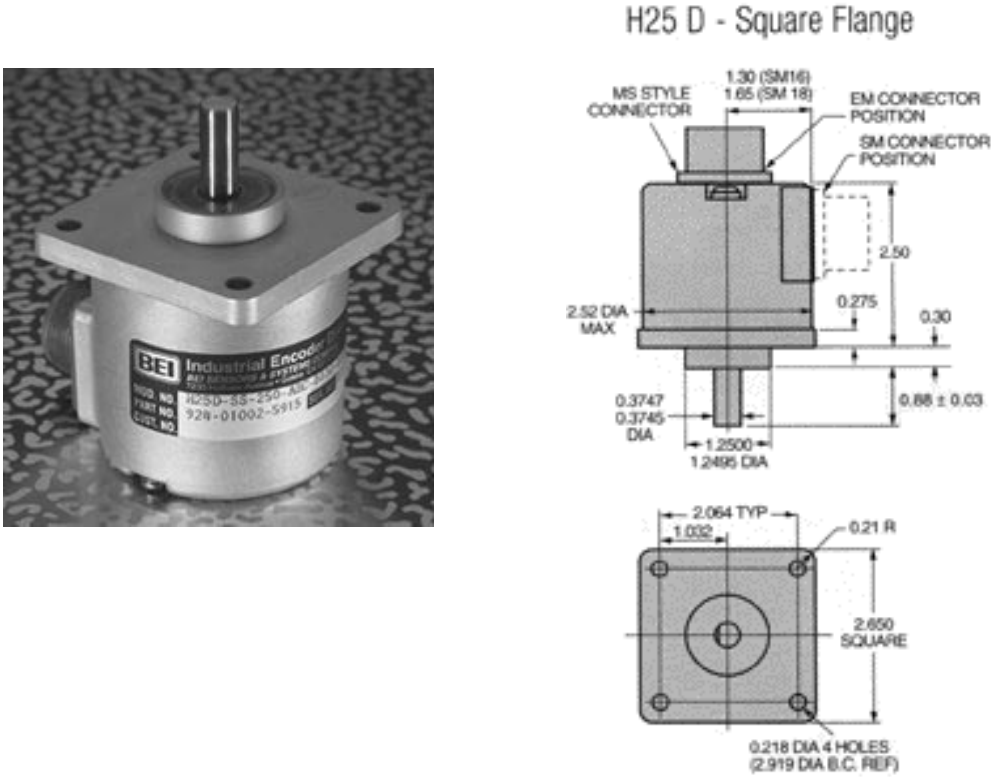

Figure 30 – Typical Optical Encoder

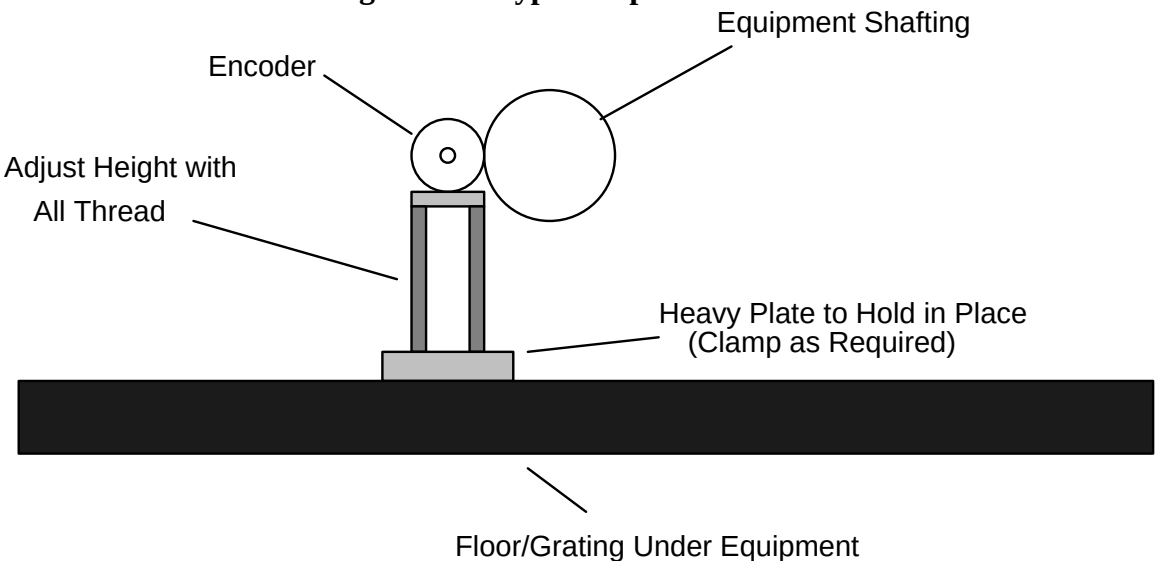

Figure 31 – Encoder Mounting Using Flexible Elements such as All-Thread

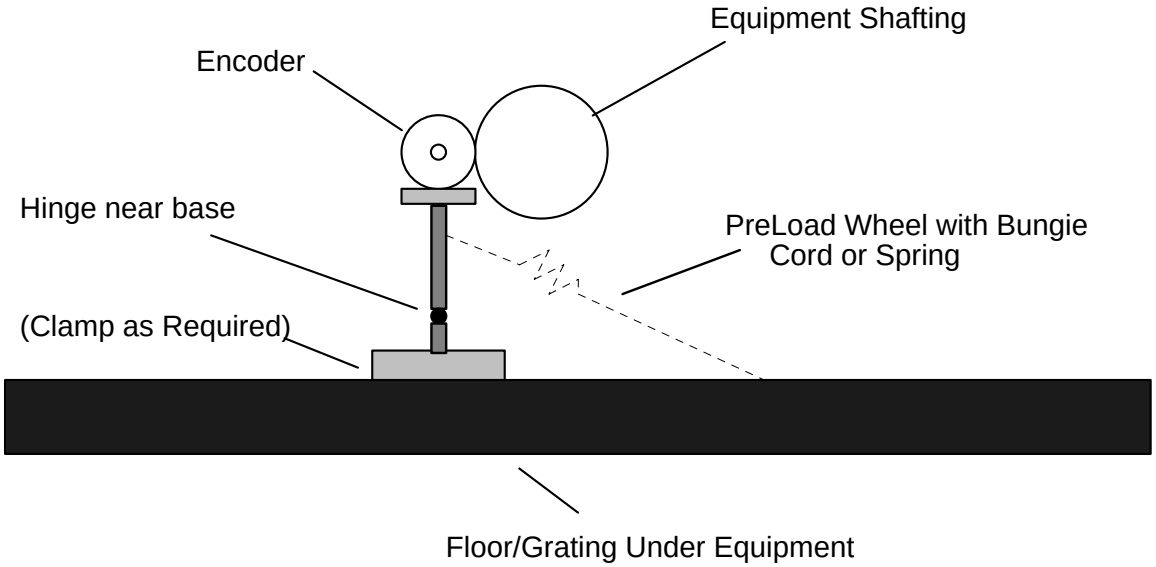

Figure 32 – Encoder Mounting Using a Hinged Joint and Bungee Cord

When the encoder is properly mounted and in good rolling contact with the shaft, the signal is demodulated with the same torsional demodulation circuitry used with the proximity probe method. A typical arrangement for the required test equipment is shown in Figure 33. An actual encoder mounting using the hinged plate method is shown in Figure 34.

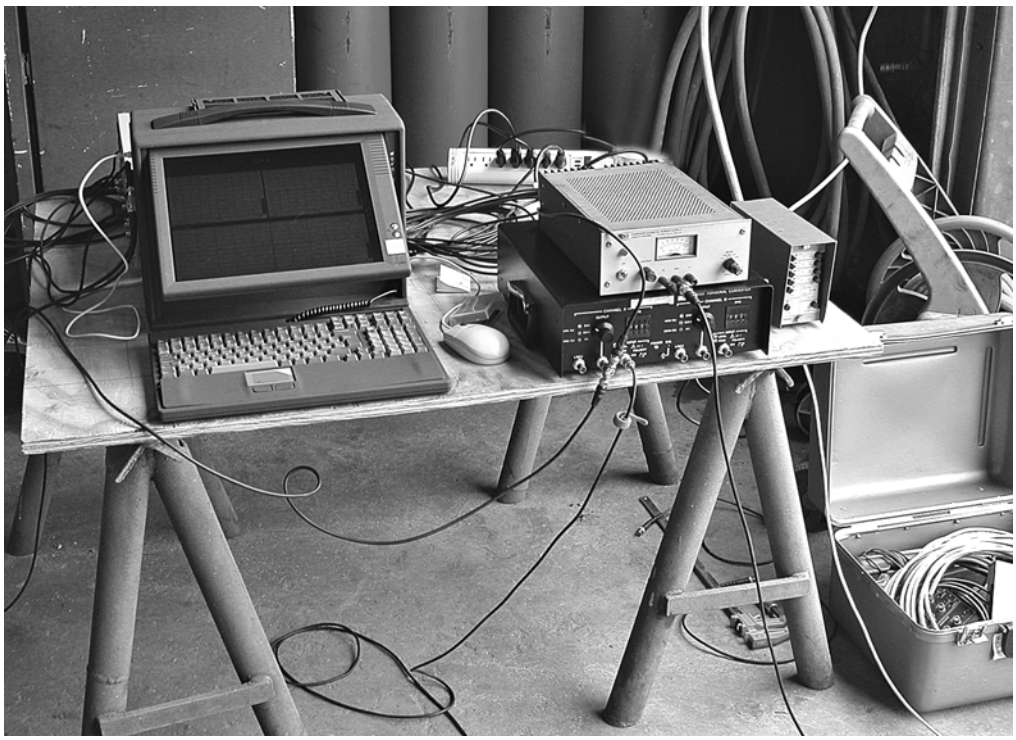

Figure 33 – Typical Test Equipment Setup for Optical Encoder Method

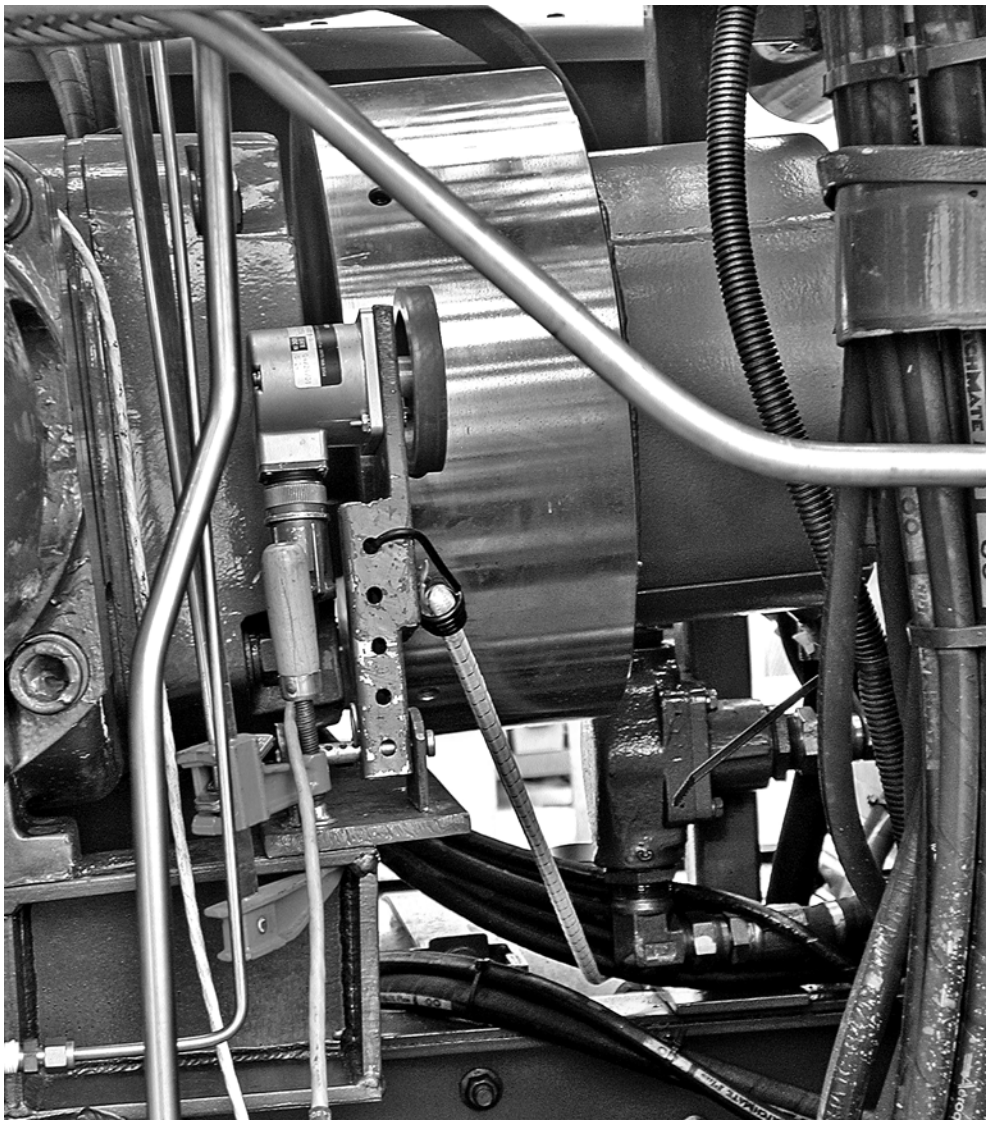

Figure 34 – Example Mounting of Encoder Using Hinged Plate

Direct Measurement of Shaft Strain: When direct shaft stress measurements are required as opposed to just measuring torsional amplitude, the torsional shear stress on the shaft surface can be determined [10, 11]. Shaft stress cannot be measured directly. However, if properly done, shear strain can be measured and used to estimate the shear stress using common stress-strain relations.

Strain measurement is done by mounting a series of strain gages on the shaft surface, with the gages mounted in a pattern where the gages are all 45° from the axis of the shaft. Figure 35 shows the typical strain gage pattern including a dual 90° rosette. The gage shown in Figure 35 would generally be about ½" tall and 3/8" wide, and be provided with solder pads for mounting the leads.

To minimize the influence of other shaft loadings such as bending or axial force, the gage rosette shown in Figure 35 is normally mounted in pairs on opposite sides of the shaft at the same axial location. The wiring connection to the pair of gages is shown in Figure 36, where the gages are shown as if the surface of the shaft has been unrolled into a flat plane. Using this method, a strong signal can be generated that has little influence from other loading such as shaft bending.

Description Two-element 90° rosette for torque and shear-strain measurement. Sections have a common electrical connection.

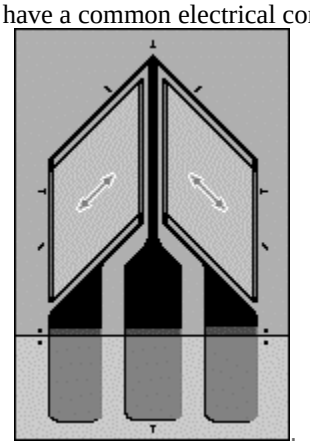

Figure 35 – Typical Strain Gage for Torsional Measurement

If shaft is "unrolled" so that both gages are viewed as from above the gage looking toward the shaft, gages should be interconnected as follows:

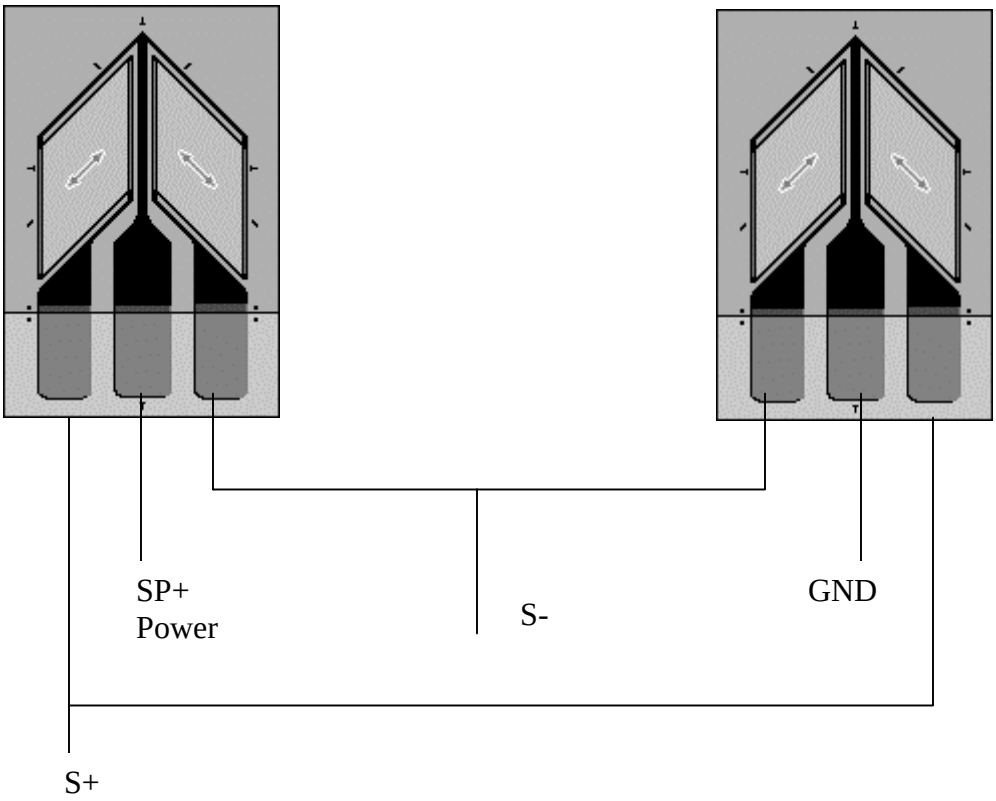

Figure 36 – Strain Gage Wiring for Dual 90° Rosettes for Torsional Strain Measurement

Once the gages are properly mounted, they must be powered and provided with a method for transmitting the strain signals off the rotating shaft. The gage power can be provided either using a battery powered device (short term test) or an inductive powered device. Wireless hardware is currently available from a number of suppliers that can transmit the strain levels quite successfully.

Figure 37 shows a typical mounting arrangement on a shaft section along with the bridge arrangement.

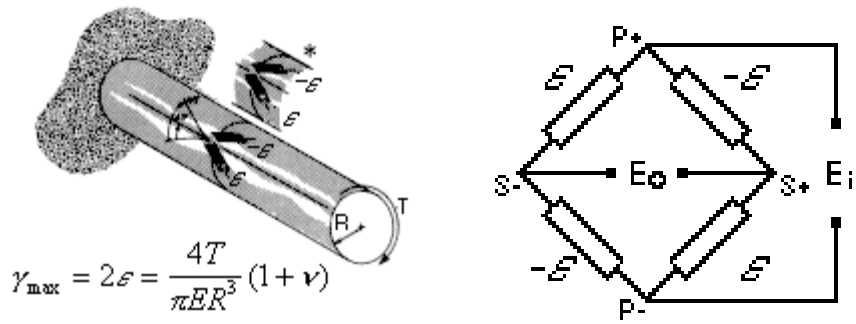

Figure 37 – Gage Mounting and Bridge Description

Indirect Measurement Methods: It is also possible to measure torsional vibration response by using indirect methods such as motor current loading and radial vibration in some limited cases. However, prediction of the amplitudes from these indirect methods will require a considerable modeling effort to assure that the relationship between the measured value and actual torsional response is accurately known.

Radial Vibration: Torsional vibration will couple into radial vibration at gear elements [10]. This coupling is one of the major sources of torsional damping by flexing of the bearing oil film when hydrodynamic bearings are located on the gear elements. When adequate amplitudes of torsional vibration are present, the gear elements will react to the dynamic torque by moving in the direction of the dynamic torque on the gear teeth.

Response of the gear rotors can be easily measured using proximity type probes that are mounted in the direction of torque loading on the gear teeth. However, the amplitude of response will generally be rather low, making identification of torsional vibration difficult without a detailed torsional analysis. Measuring the radial vibration during a coastdown of a gearbox can be an effective method for verifying torsional natural frequencies [11].

Motor Amps: In some cases, where torsional vibration is severe, the presence of torsional vibration can be done by measuring the variation of the current signal feeding the motor driving the equipment. This method is very indirect, but can be used to verify torsional vibration in severe cases.

Motor amps can be observed to swing dramatically for a reciprocating pump or compressor where the heads are not well balanced or timed. In these cases, the torsional vibration will often occur at 1X RPM of the pump, which is often less than 200 CPM (3.3 Hz). For extreme cases, this can be observed on analog ammeters or measured with a high speed recording device. However, correlation with actual torsional vibration (amps/deg) would have to be determined for the specific system to allow prediction of actual torsional vibration levels.

Calibration: Any measurement system would not be useful without some method of calibration or verification that the instruments are producing accurate results. Torsional vibration can be difficult to verify or validate without a torsional calibrator.

One well accepted version of calibrator is shown in Figure 38. This device uses a standard Hooke's joint type coupling (universal joint) to produce predictable torsional vibration amplitude at the test sensor. The Hooke's joint will produce a predictable torsional oscillation at 2X RPM of the driven shaft. For the calibrator to be effective, the motor must have significantly more rotary inertia than the drive shaft and sensor so that the torsional vibration of the sensor is not producing torsional vibration reaction at the motor, making the calibrator output erroneous.

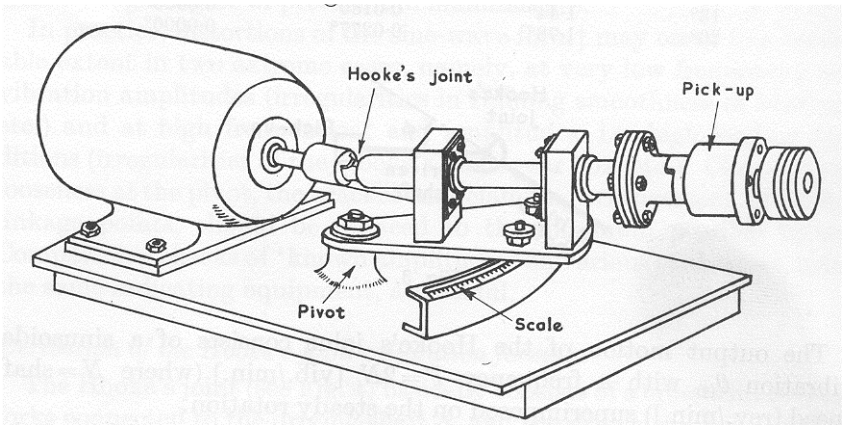

Figure 38 – Torsional Calibrator

Strain gage methods can also be calibrated during testing, but not by using a calibrator as shown in Figure 38. The strain gage method is calibrated on the actual test shaft by using a shunt calibration resistor applied across the individual elements of the strain gage. Predictable response of the output can be calculated and used to verify the output levels from the measuring instrumentation.

Case History 1 – Triplex Pump: The first case history presented includes the torsional vibration response of a cryogenic pump used in oil well servicing. The pump tested was a triplex pump using liquid nitrogen as the pumped liquid. The torsional vibration testing followed the torsional analysis for the truck system shown in Figure 24.

Excessive torsional vibration was expected due to damage of internal flywheels and keyways on the pump crankshaft. Other damage suggestive of high torsional vibration amplitudes was also present including unusual wear on both sides of the gear teeth.

Torsional vibration was measured using an optical encoder with a measuring wheel attached mounted at the input end of the pump. The wheel was positioned to roll against the coupling hub outside diameter on the original test, then against the flywheel that was added in the final test. The mounting of the encoder is shown in Figure 34 for the final test with the installed flywheel.

The results of the torsional vibration measurement are shown in Figures 39 and 40. The high torsional vibration at 2X RPM was caused by high offset angles in the universal joint type drive couplings used between the transfer case and the pump. Angular offset angles near 9° were used. The high reaction at 3X RPM was expected due to the triplex pump arrangement (three heads per pump), and was strongly dependant on pump loading.

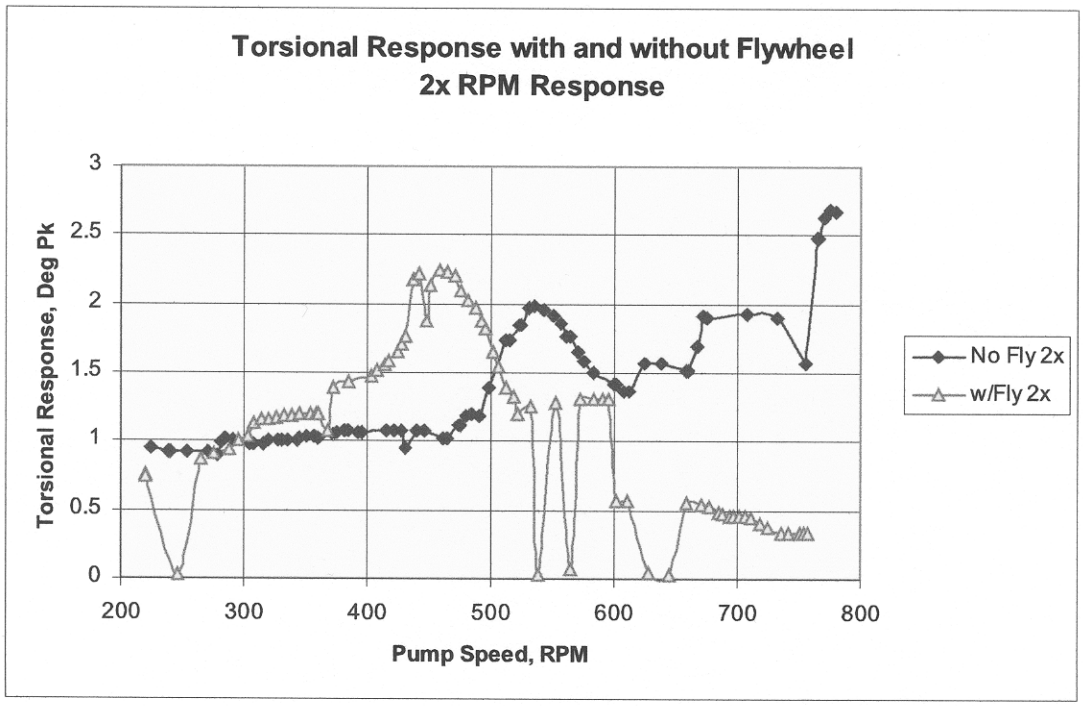

Figure 39 – Torsional Vibration Response at Pump Input Shaft at 2X RPM

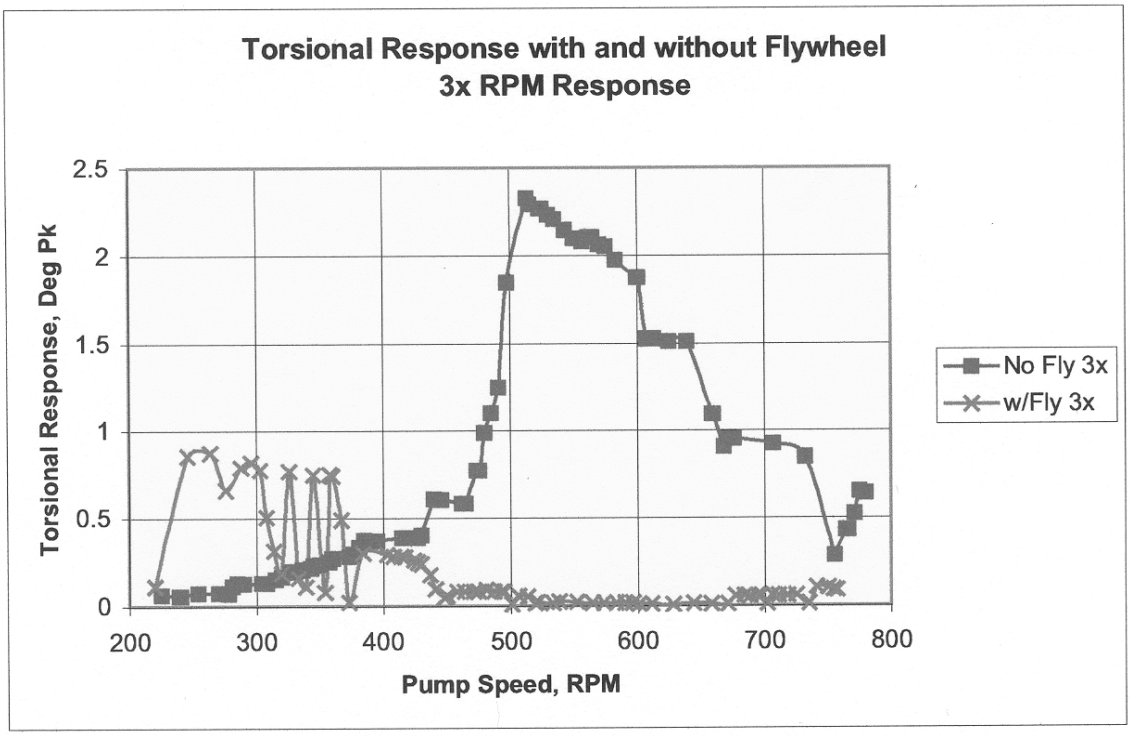

Figure 40 – Torsional Vibration Response at Pump Input Shaft at 3X RPM

Case History 2 – Cooling Tower Fan: The second case history includes torsional vibration response of a cooling tower fan. A fan sketch is shown in Figure 41, and is typical for a cooling tower fan.

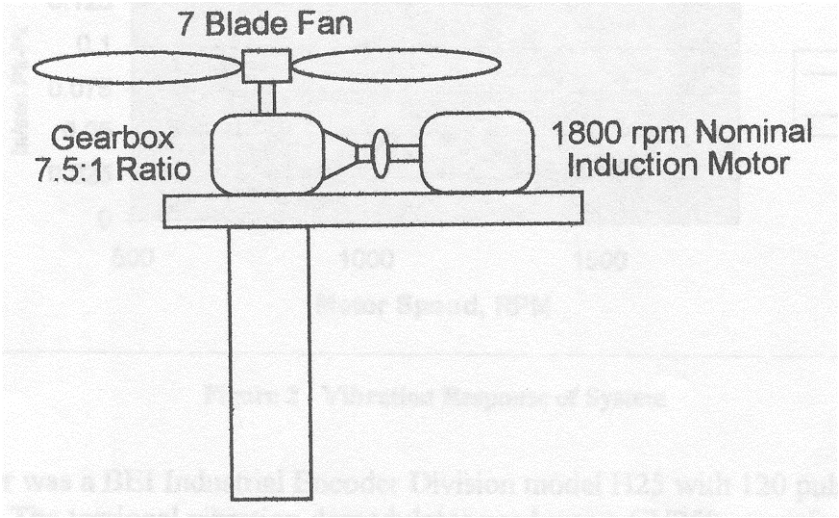

Figure 41 – Cooling Tower Fan Arrangement

The problem with the application was premature wear and damage of the gear teeth in the right angle gear. In particular, heavy wear was obvious on both sides of the gear teeth.

The vibration data recorded on the unit included both radial and torsional vibration. Radial vibration was measured at numerous locations on the motor and gearbox, and torsional vibration was measured on the motor end of the drive coupling using an optical encoder and measuring wheel. The radial vibration is shown in Figure 42, and the torsional vibration is shown in Figure 43. As observed in Figure 42, the torsional vibration couples into radial vibration at the torsional resonance. However, this reaction could not be identified as a torsional resonance without torsional analysis and torsional vibration measurement.

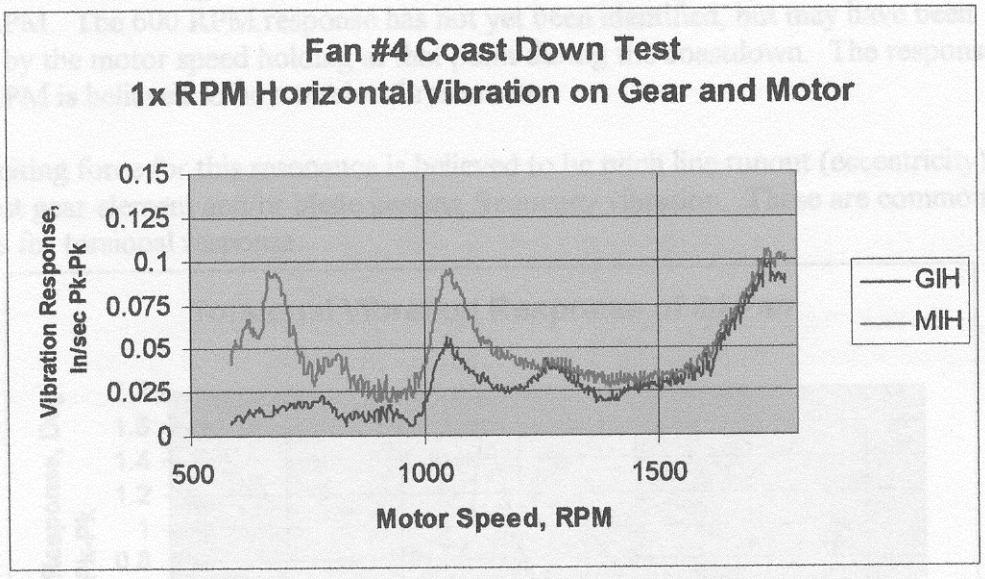

Figure 42 – Cooling Tower Radial Vibration

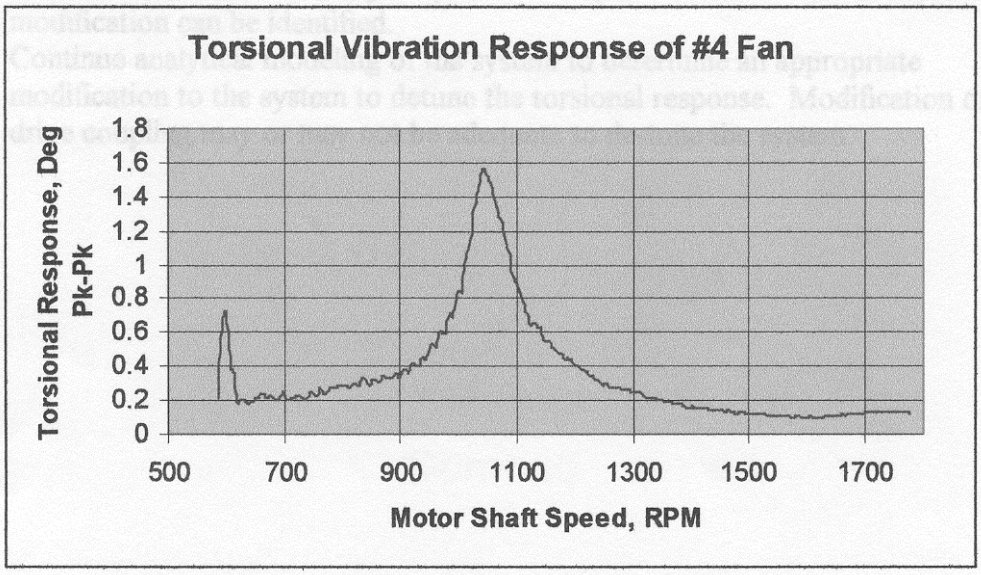

Figure 43 – Torsional Vibration at Motor

The torsional vibration near 1040 RPM was determined by modeling to be caused by a torsional resonance in the system, which was later corrected by replacing the drive coupling.

Case History 3 – Synchronous Motor Start: Synchronous motor starts can produce high torsional vibration amplitudes as described above. This case involves a synchronous motor driving an integral gear multistage air compressor. The air compressor has a large bull gear and two high speed pinions with impellers on each end of each pinion.

The system was instrumented with both a shaft strain measuring system at the drive coupling and also instrumented with optical encoders using the measuring wheel method. Output from each measurement method was recorded using a digital data acquisition system.

Response of the torsional vibration measurement using the optical encoder for a motor start is shown in Figure 44. The peak torsional vibration occurred at a shaft speed of about 1093 RPM, which was due to a torsional resonance near 800 CPM that was excited by the torsional pulsations from the synchronous motor. In this case, the torsional vibration was so extreme, that the proximity probes mounted in the compressor pinion bearing on one shaft rubbed due to excessive wear/failure of the bearing on the pinion.

Since the torsional vibration was high and the proximity probe was damaged, the bearings were removed for inspection. The pads in the bearing with the highest vibration reaction are shown in Figure 45. The lower pads can be observed to have obvious damage, even though the machine only ran for about 20 seconds. It is believed that this damage occurred during the torsional resonance, and was caused by torsional/lateral coupling between the pinions and the bull gear.

The response of the shaft strain telemetry system is shown in Figure 46 with the output converted to shaft torque. The dynamic torque during the torsional resonance was found to be quite high, as suggested by the radial response of shaft probes and damage to the pinion bearings. Both the torsional vibration and the shaft torque measurements produced similar results, which could be compared using a torsional analysis model. A waterfall plot for the radial vibration at the failed bearing is shown in Figure 47.

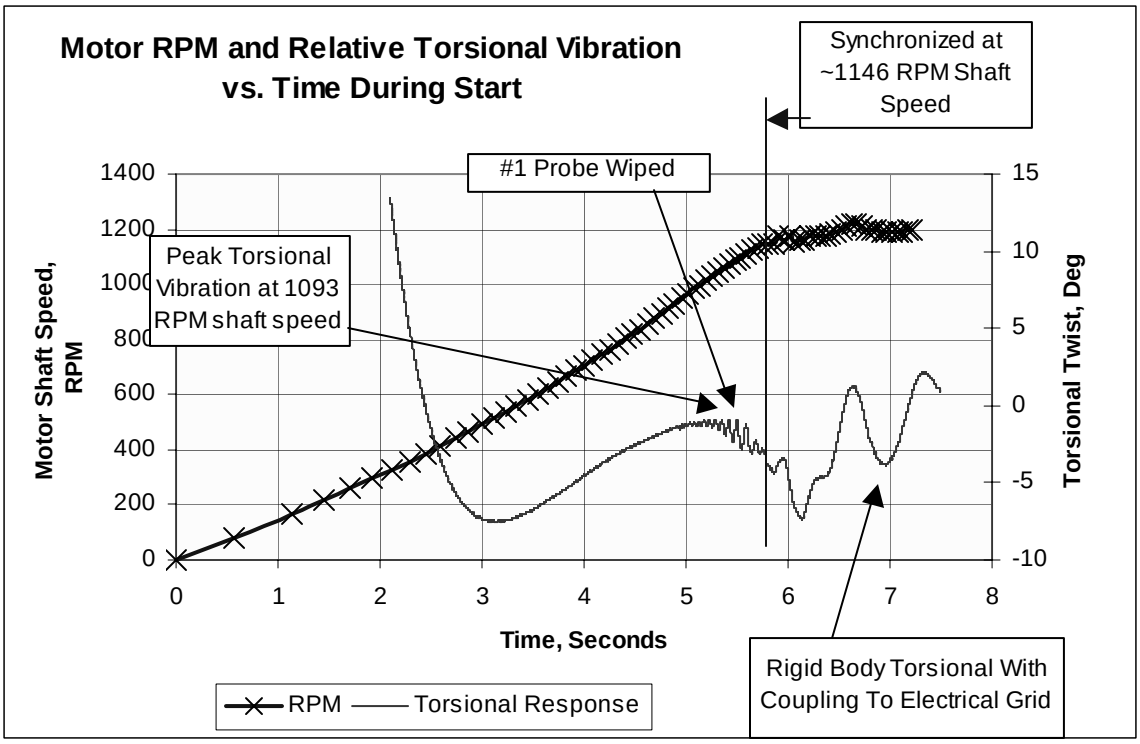

Figure 44 – Torsional Vibration Response of Synchronous Motor

Figure 45 – Damage on Bearing Pads After Initial 20 Second Run

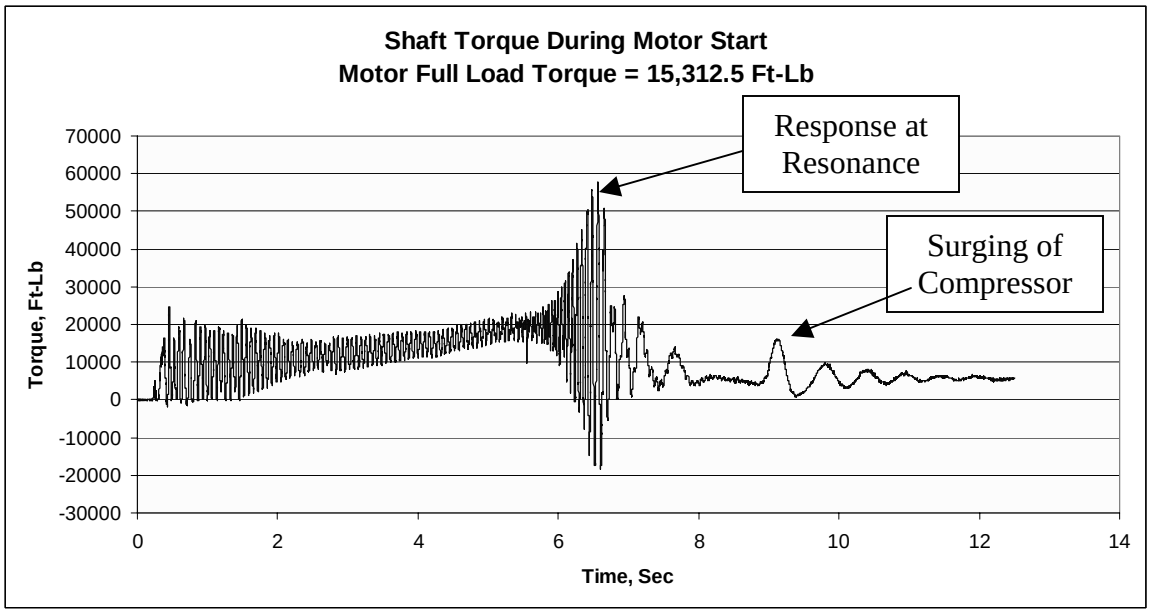

Figure 46 – Dynamic Shaft Stress during Motor Start

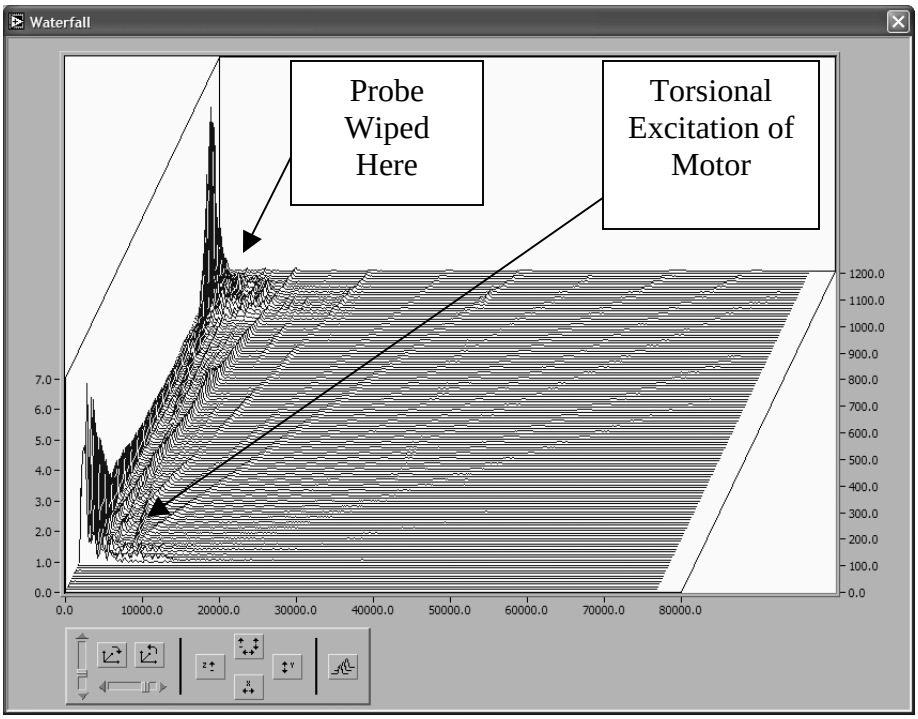

Figure 47 – Waterfall for Radial Probe at Failed Bearing

Case History 4 – Locomotive: Torsional vibration of reciprocating engines can be a significant cause of crankshaft failure if not properly addressed. Testing was completed on a 16 cylinder Vee engine driving a generator on board a locomotive. The purpose of the testing was to verify the torsional analysis results, which suggested some rather high torsional response at a 2.5X engine order.

Four cycle diesel engines produce harmonic response at all ½-order harmonics including ½X, 1X, 1½X, 2X, …. 11½X, 12X and higher. Each engine design and firing order will have certain harmonics that produce higher amplitudes than others. Each of these orders will often pass through torsional resonance frequencies at some engine speed.

The system was instrumented with several optical encoders, including on the free end of the engine shaft and at the load coupling to the generator. The torsional response at the engine end is shown in Figures 48 and 49, with the orders separated at each engine speed.

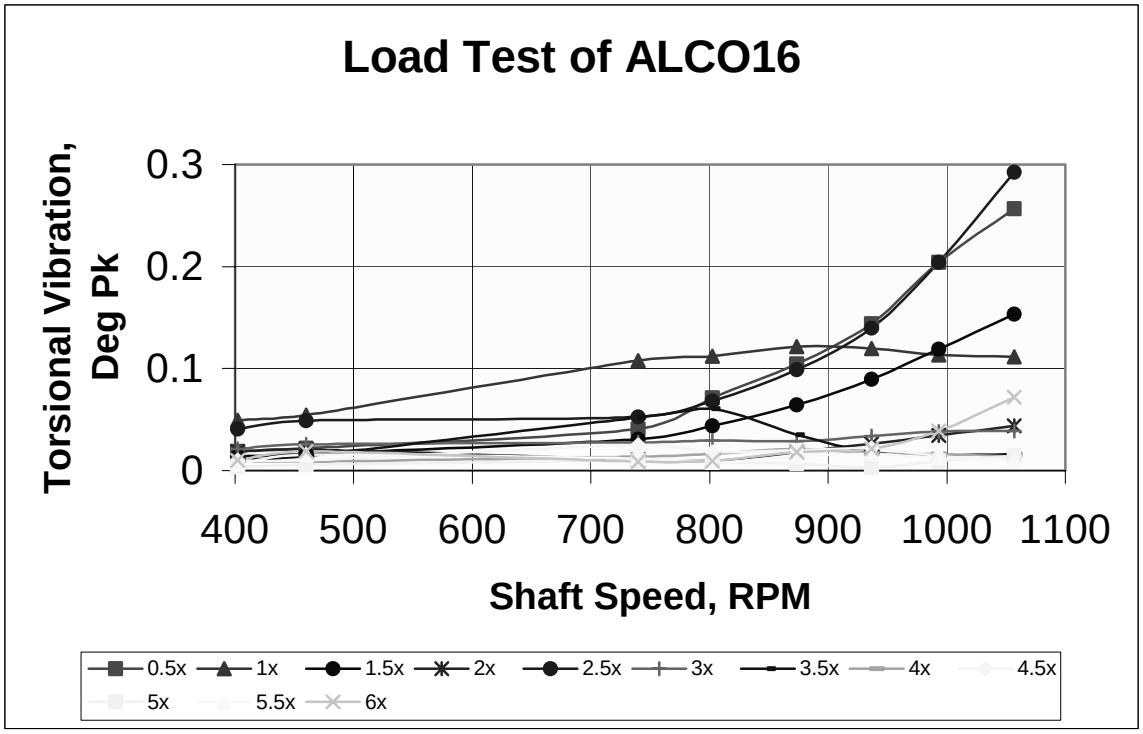

Figure 48 – ½ to 6X Orders of Engine Speed

The response data for each engine order along with the results of a torsional analysis model were used to calculate combined dynamic shaft stress values using the method described in B.I.C.E.R.A. [1]. The combined stress amplitude for the most heavily loaded crank section is shown in Figure 50.

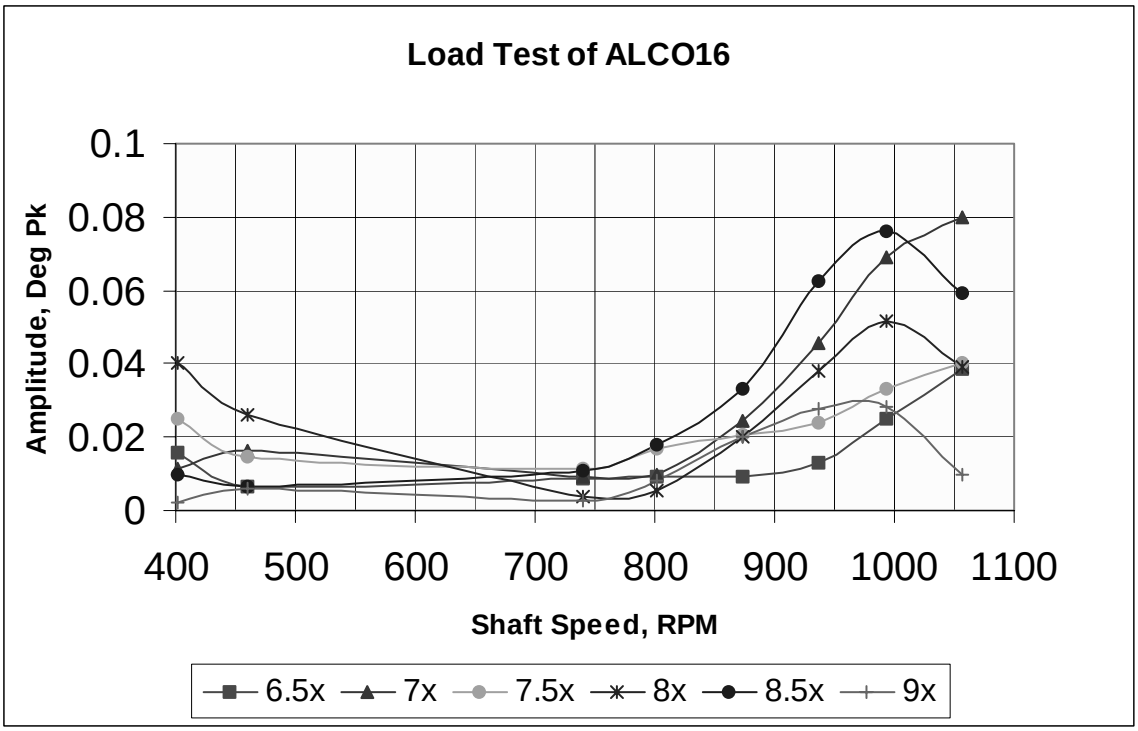

Figure 49 – Torsional Response at 6.5X to 9X RPM of Engine

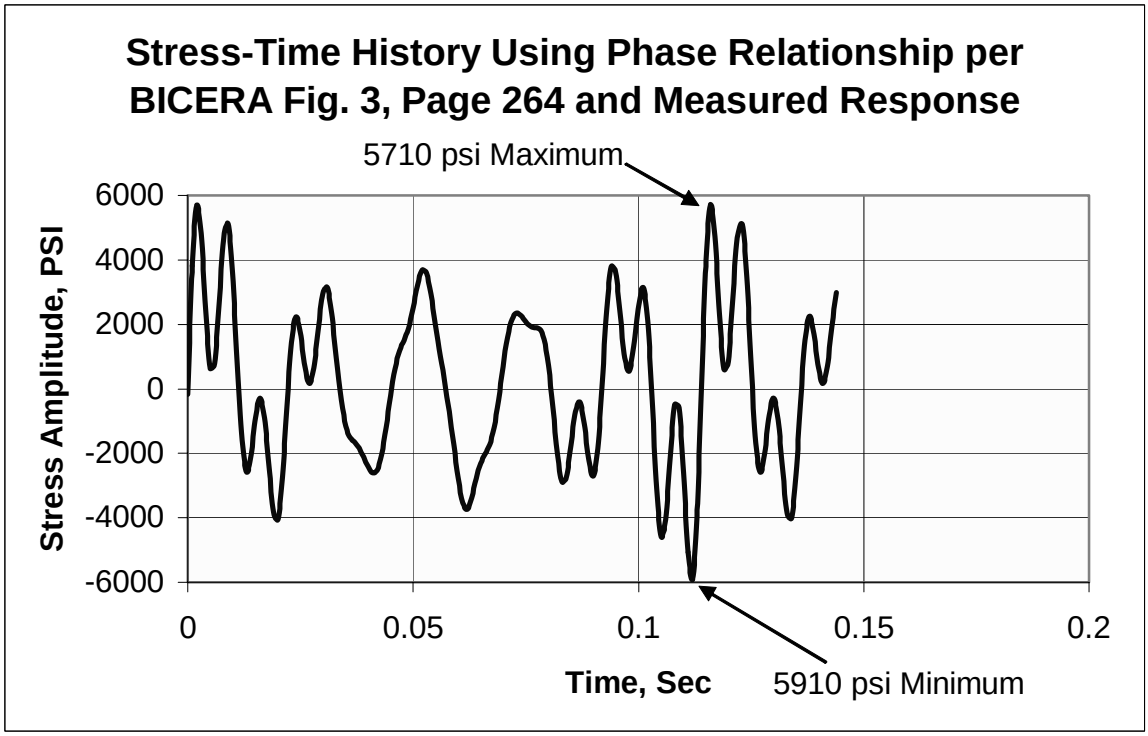

Figure 50 – Combined Torsional Stress due to All Measured Engine Orders

Case History 5 – Tractor Engine Auxiliary Fan Drive: Failures were occurring on some auxiliary fans mounted on a tractor engine. Torsional failure modes were expected, and torsional vibration testing of the engine and fan was completed. The engine was instrumented using optical encoders and measuring wheels as shown in Figures 51 and 52. One encoder was mounted against the engine crankshaft and one on the fan of concern.

Figure 51 – Optical Encoder at Crankshaft

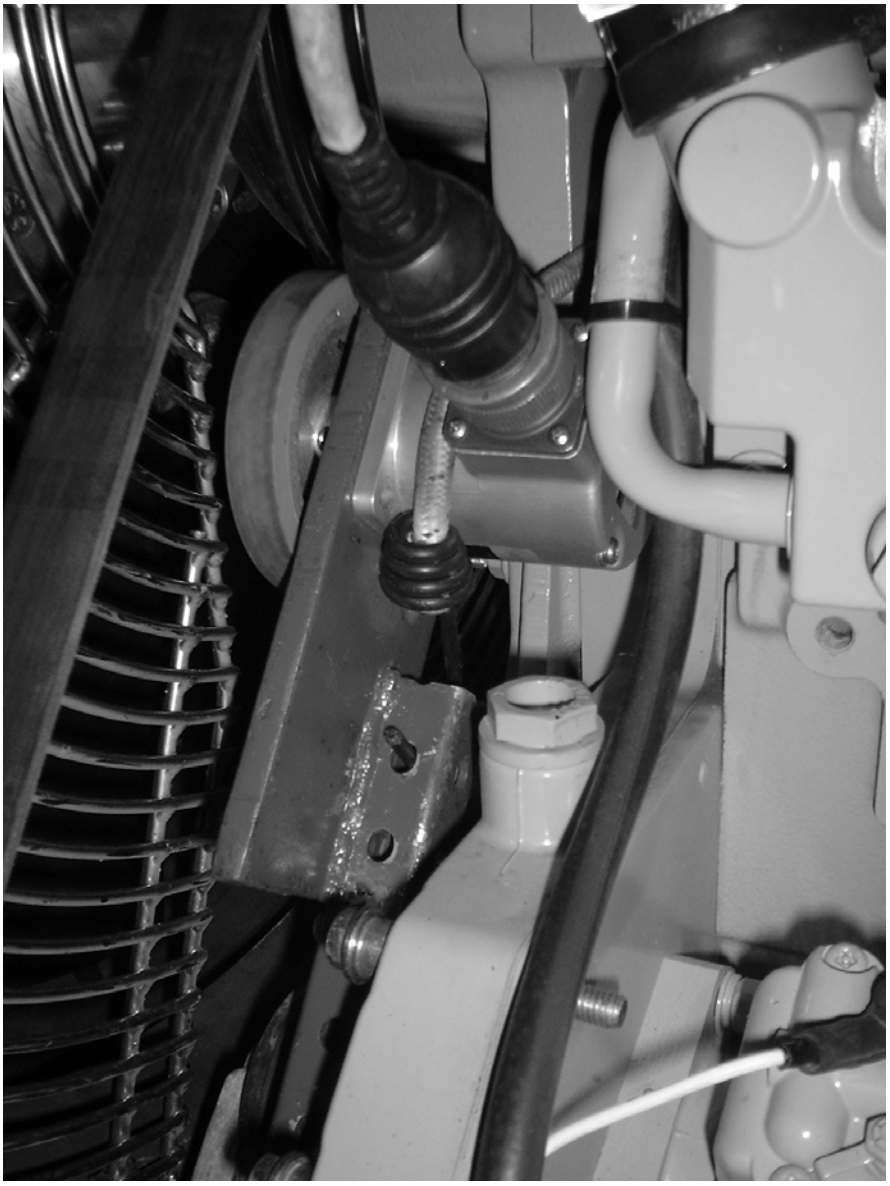

Figure 51 – Optical Encoder Mounting on Fan Drive Sheave

The torsional response of the engine and fan unit is shown in Figure 52. As expected, the torsional vibration of the crankshaft is much higher than the general response of the belt driven auxiliary fan.

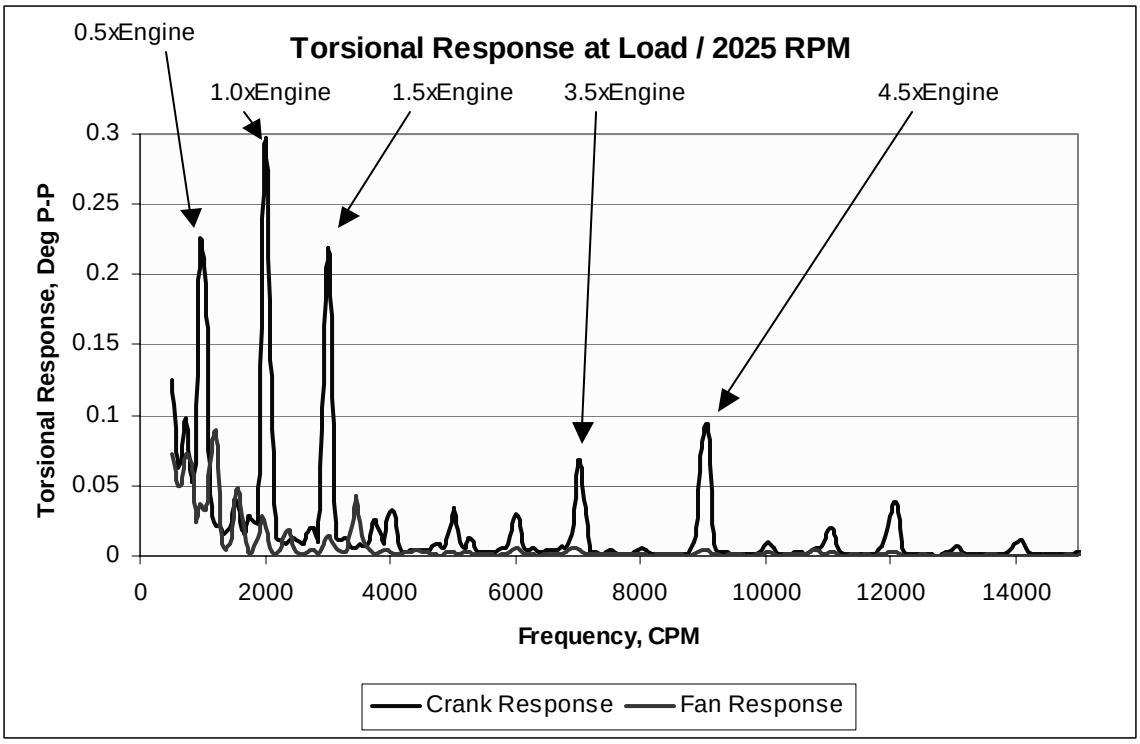

Figure 52 – Torsional Vibration of Tractor Engine and Fan

Conclusion: Torsional analysis and torsional measurement are as intimately related as an artist and his canvas. One can exist without the other, but only when they are combined is the full picture revealed. Taking a shot at torsional measurement without some knowledge of the torsional frequencies and mode shapes is as likely to lead to the wrong conclusion as the right one.

Lateral vibration is easy to measure and difficult to predict. Torsional vibration is difficult to measure and easy to predict. The finite element modeling methods shown in this paper allow the analyst and the designer to put together a reasonably accurate but "crude" model that will act as a good guide to the best methods and locations for field measurement of torsional twist amplitudes and/or shaft strain. The initial field tests are then fed back into the model for fine tuning and greater accuracy. Once there is high confidence in the refined model, it is possible to propose changes and test theories that will solve complex problems without the expense of fabricating the hardware until the best fix is determined. Often there are numerous ways to alter the torsional resonances in a machine train and only one will be practical or economical.

This paper has presented the basic theory behind torsional analysis and measurement. Numerous real examples have been shown that were solved by applying the principals in this paper. There is a wealth of additional information in the literature. Unfortunately, two of the best references (1 and 4) are no longer in print. The authors have found copies of these books at on-line sources and in used bookstores. Any serious torsional investigator is urged to locate their own copies. Reference 2 is the newest book available on torsional analysis and would be a valuable addition to any engineer's library.

Acknowledgements: The authors wish to thank Dr. Wen Jeng Chen, the author of the DyRoBeS finite element analysis program used to produce the analyses and analytical plots. In addition, thanks go out to Dr. Ed Gunter and Charlie Jackson for continued inspiration and to the Vibration Institute for publishing this work.

References:

1. Nestorides, E. J., B.I.C.E.R.A. *Handbook of Torsional Vibration*, Cambridge University Press, 1958

2. Walker, Duncan N., *Torsional Vibration of Turbomachinery*, McGraw-Hill, 2003 ISBN 0-07-143037-7

3. Corbo, Mark A. And Melanoski, Stanley B., *Practical Design Against Torsional Vibration*, Tutorial, 25th Texas A&M Turbomachinery Symposium pp 189-222, September, 1996

4. Ker Wilson, W., *Practical Solution of Torsional Vibration Problems*, Volumes 1 through 5, John Wiley & Sons, 1959

5. *Tutorial on the API Standard Paragraphs Covering Rotor Dynamics and Balancing: An Introduction to Lateral Critical and Train Torsional Analysis and Rotor Balancing*, API Publication 684, February, 1996

6. Jackson, C. And Leader, M.E., *Design and Commissioning of Two Synchronous Motor-Gear-Air Compressor Trains*, 13th Texas A&M Turbomachinery Symposium, November, 1983.

7. API 613, 5th Edition, "Special Purpose Gear Units for Petroleum, Chemical, and Gas Industry Services", American Petroleum Institute.

8. Holdrege, J., Subler, W., and Frasier, W., "AC Induction Motor Torsional Vibration Consideration – A Case Study", IEEE Transactions on Industry Applications, Vol. 1A-19, No.1, Jan/Feb 1983.

9. Simmons, H. and Smalley, A., "Lateral Gear Shaft Dynamics Control Torsional Stresses in Turbine Driven Compressor Train", ASME paper 84-GT-28 presented at the 29th International Gas Turbine Conference and Exhibit, June 1984.

10. Vance, J. and French, R., "Measurement of Torsional Vibration in Rotating Machinery", ASME paper 84-DET-55 presented at the Design Engineering Technical Conference, June 1984.

11. Simmons, H, and Smalley, A., "Effective Tools for Diagnosing Elusive Turbomachinery Dynamics Problems in the Field", ASME paper 89-GT-71 presented at the Gas Turbine and Aeroengine Congress and Exhibition, June 1989.

12. Dashefsky, G.J., "The Elimination of Torsional Vibration," The third national meeting of the Oil and Gas Power Division of ASME, Penn State College, June 14, 1930.